IEEE Access
Multidisciplinary | Rapid Review | Open Access Journal

Received 8 March 2023, accepted 17 March 2023, date of publication 20 March 2023, date of current version 23 March 2023.

Digital Object Identifier 10.1109/ACCESS.2023.3259732

SURVEY

Design and Performance Evaluation of OAM-Antennas: A Comparative Review

OMAR A. SARAEREH
Department of Electrical Engineering, Faculty of Engineering, The Hashemite University, Zarqa 13133, Jordan
e-mail: eloas2@hu.edu.jo

This work was supported by the Deanship of Scientific Research at The Hashemite University.

ABSTRACT For many communication systems, including wireless networks, mobile, satellite, radar, remote sensing, and many more applications, antenna arrays are very necessary. Utilizing effective beamforming techniques, antenna arrays have recently played a major part in driving data rates and system capacity to extremely high levels. The beamforming capabilities and system performance are both greatly influenced by the array configuration. Numerous array structures, including linear, two-dimensional, circular, conical, cylindrical, spherical, and even non-uniform array shapes, can be used in different applications. Modern communication systems pay a lot of attention to reconfigurable antennas because of the many applications they may serve and the added functionality they provide. A single structure that has the ability to change between one or a number of features, such as frequency, pattern, and polarization, is referred to as a reconfigurable antenna. Utilizing a specific circular phased microstrip antenna array, the orbital angular moment (OAM) vortex electromagnetic wave is created, allowing for more effective and dependable data transmission. When propagating, the vortex electromagnetic wave has a spiral phase wavefront structure, and its many OAM modes are orthogonal to one another. The helical antenna offers the benefits of light weight, small size, and excellent circular polarization when compared to other OAM radio producing techniques. This paper reviews various state-of-the-art antennas for 5G applications. Specifically, the single microstrip, array, traveling wave and metasurface antennas have been discussed and their important aspects were elaborated. Finally, the applications and future prospects were described.

INDEX TERMS OAM antennas, array, beamforming, electromagnetic waves.

I. INTRODUCTION

The fixed frequency band bandwidth increasingly restricts the growth of wireless communication technology due to the rapid advancement of science and technology in contemporary society and the steadily rising number of wireless communication users. Therefore, scholars have conducted a lot of research and exploration in order to achieve higher frequency utilization. Due to its infinite mode and orthogonality across modes [1] and its importance for increasing channel capacity, orbital angular momentum (OAM) has received a lot of interest from researchers in recent years. The beginning of mankind's understanding of OAM comes from the field of optics. Recently, various new approaches were proposed to model the antennas, in which ChatGPT has important role. The author in [2] theoretically predicted the mechanical effect of spin angular momentum related to circularly polarized electromagnetic fields. After that, reference [3] were experimentally verified. References [4] and [5] proposed and developed concepts such as phase dislocation, phase singularity, and vortex beam, and then conducted further research [6], [7], [8], [9], [10], gradually enriching the theory, generation, and related properties of vortex light. Reference [11] found that the vortex laser beam formed by Laguerre-Gauss (LG) beams had orbital angular momentum, and clearly determined the relationship between orbital angular momentum and vortex topological charge the relationship between. Since then, several research groups have worked on various optical vortex generation schemes [12], [13], [14], [15], [16], optical vortex manipulation of micro-nano particles [17], [18], [19],

The associate editor coordinating the review of this manuscript and approving it for publication was Giorgio Montisci.

This work is licensed under a Creative Commons Attribution-NonCommercial-NoDerivatives 4.0 License.
For more information, see https://creativecommons.org/licenses/by-nc-nd/4.0/

[20], [21], vortex optical micromachining [22], photon orbital angular momentum quantum entanglement properties [23], [24], [25], optical vortex propagation properties [26], [27] etc. At the same time, because the OAM state (vortex topological charge) in the vortex beam has infinite value possibilities and mutual orthogonality, it can provide a new type of physical freedom for the optical communication system, which is considered to be a very important research direction for the next generation optical communication network. In recent years, the OAM multiplexing system has shown good performance in expanding the channel capacity of the optical communication system [28], [29], [30]. At the same time, in the field of wireless communication, there is also an application demand for channel capacity expansion. Therefore, many scholars believe that the OAM multiplexing system should also have the characteristics and great potential of expanding channel capacity in radio frequency wireless communication systems, and launched a series of researches on this. In reference [31] for the first time, the experiment of wireless communication based on two different modes of OAM was successfully realized in the radio frequency band. Since then, how to better apply OAM to the field of wireless communication has been the research focus of many researchers [32], [33], [34]. The vortex electromagnetic wave antenna not only has broad application prospects in the field of wireless communication, but also has great potential application value in radar imaging and detection. The imaging method uses vortex electromagnetic waves to achieve super-resolution of target imaging in the azimuth direction, which can provide a new technical approach for super-resolution radar imaging. Since then, in order to improve the imaging resolution and expand the imaging dimension, domestic scholars have proposed some improvement measures of the radar imaging algorithm based on the vortex electromagnetic wave antenna [36], [37], [38]. The rotating Doppler effect of vortex electromagnetic waves can realize the efficient detection of target rotation speed, and a series of experiments have also verified the feasibility of this method [39], [40]. In addition, some scholars have also begun to combine vortex electromagnetic wave antennas with medical Imaging combined as a novel means of disease detection [41].

All applications of vortex electromagnetic waves must be based on the existence of the required vortex electromagnetic waves, so how to efficiently generate the required vortex electromagnetic waves is the research basis in this research field. In recent years, many researchers have proposed various methods are used to generate vortex electromagnetic waves in the radio frequency range. Reference [42] used a spiral phase plate to generate vortex electromagnetic waves in the millimeter-wave (mmWave) band for the first time. Reference [43] proposed to use a circular array antenna phase modulation method to generate radio frequency of vortex waves extends the research of vortex electromagnetic waves to lower the frequency bands. Reference [44] have summarized the basic theory, propagation and application of vortex electromagnetic waves. Reference [45] proposed a dual-polarized and reconfigurable reflectarray for generation of OAM vortex electromagnetic wave. It generates 25 combinatios of OAM modes reconfigurably by changing capacitance values of varactors.

This paper makes a more comprehensive summary of OAM vortex electromagnetic wave antennas in the radio frequency field, primarily introducing four distinct antenna types that produce vortex electromagnetic waves, including active single microstrip patch antennas, travelling wave antennas, array antennas, and passive metasurface antennas, each of which is intended to produce OAM electromagnetic waves with a variety of properties. Due to its small size, inexpensive manufacture, and relatively straightforward structure, a single microstrip patch antenna has attracted the attention of researchers who are interested in producing vortex electromagnetic waves. Traveling wave antennas can generate vortex in multiple OAM modes in a broadband range, and this advantage can just meet the requirements of the communication system to expand the channel capacity. In order to make the system more practical, many researchers have also carried out a lot of research in the field of traveling wave antennas. Array antennas are now used on aircraft and radar and is one of the most widely used antenna types [46], [47], [48]. It is also the main way to generate OAM in the radio frequency band. Through feeding, the switching of multiple OAM states can be realized, but the difficulty of this design lies in its complicated feeding network. Many researchers have done some research on this kind of phased array feeding network design and optimization work has been completed. The metasurface is composed of metamaterial resonators arranged periodically in sub-wavelength size, and it can realize sudden changes in the amplitude or phase of electromagnetic waves by changing the shape and size of the resonators, and by rationally arranging the metamaterial resonators in space. The surface structure can effectively generate and control vortex electromagnetic waves. Compared with the traditional phased array antenna, the metasurface antenna has the advantages of low profile, simple feeding system and easy beamforming [49], but there are a large number of array elements, complex structural design and bulky volume, etc., still need further optimization and research.

In short, with the continuous deepening of research on vortex electromagnetic wave antennas, the antenna structure in the radio frequency band is simple, the overall profile is low, easy to integrate, and can generate multiple modes of OAM at the same frequency. This essay's material is separated into four sections. The introduction is the first section and it provides a summary of the history, evolution, and current trends in vortex electromagnetic wave applications. The second section compares vortex electromagnetic waves to OAM and explains its theoretical foundation. The connection between them is discussed, and the fundamental idea and properties of orbital angular momentum are provided. The technique for creating vortex electromagnetic is examined in

the third part. It summarizes the benefits and drawbacks of each type of antenna before summarizing and anticipating future advancements based on these four types of antennas. Part four briefly summarizes the future application prospects of vortex electromagnetic wave antenna technology, and the key points and difficulties in the future of this research field.

II. THEORETICAL BASIS OF VORTEX EM WAVES

Radio technology has flourished due to the convenient transmission of information. With the advent of the current next generation network era and people's lives becoming increasingly informationized and intelligent, the ever-increasing number of communication services has made non-renewable spectrum resources increasingly scarce. The vortex electromagnetic wave has attracted widespread attention because it carries OAM, a new degree of freedom beyond the time domain, frequency domain, and code domain. Using this orthogonal mode can effectively improve the spectrum efficiency and communication capacity. Therefore, vortex electromagnetic waves have gradually become the focus of domestic and foreign scholars.

According to classical electromagnetic theory, electromagnetic waves not only carry energy but also momentum during transmission [50]. Similar to classical mechanics, electromagnetic angular momentum is defined as $\boldsymbol{J} = r \times P$, the density of linear momentum in the electromagnetic field can be defined as $\boldsymbol{p} = \varepsilon_0(\boldsymbol{E} \times \boldsymbol{B})$. Through the above definition of angular momentum, the equation for deriving angular momentum density can be expressed as $m = \varepsilon_0 r \times (\boldsymbol{E} \times \boldsymbol{B})$. To get the total angular momentum $\boldsymbol{J}$, it is necessary to integrate the equation of the angular momentum density, which can be obtained as:

$$\boldsymbol{J} = \varepsilon_0 \int r \times (\boldsymbol{E} \times \boldsymbol{B}) \mathrm{d}r \tag{1}$$

where, ε_0 is the vacuum permittivity, $\boldsymbol{E}$ and $\boldsymbol{B}$ represent the electric field strength and magnetic field strength, respectively. In classical mechanics and atomic physics, angular momentum can be decomposed into rotating angular momentum and OAM, namely $\boldsymbol{J} = \boldsymbol{L} + \boldsymbol{S}$, where $\boldsymbol{L}$ represents the OAM, and $\boldsymbol{S}$ represents the rotating angular momentum. They can be expressed as:

$$\begin{cases} \boldsymbol{L} = \varepsilon_0 \int \mathrm{Re}\left(i\boldsymbol{E}^*(\hat{\boldsymbol{L}}.\boldsymbol{A})\right) \mathrm{d}V \\ \boldsymbol{S} = \varepsilon_0 \int \mathrm{Re}\left(\boldsymbol{E}^* \times \boldsymbol{A}\right)) \mathrm{d}V \end{cases} \tag{2}$$

where $\boldsymbol{A}$ is the vector bit, $\hat{\boldsymbol{L}}$ can be expressed as: $\hat{\boldsymbol{L}} = -i(r \times \nabla)$. Generally speaking, the rotating angular momentum of the electromagnetic field is related to the circular polarization state, while the OAM is related to the spatial structure of the electromagnetic field (such as phase structure, polarization structure, etc.).

Reference [11] proposed the concept of photon orbital angular momentum and proved that there is a spatial phase term in Laguerre-Gaussian beams $e^{jl\varphi}$, corresponding to the OAM, and the corresponding value is $l\hbar$. The light field distribution of a typical Laguerre-Gaussian beam can be expressed as:

$$\begin{aligned} &\mathrm{LG}_{p,l}(r, \boldsymbol{\varphi}, z) \\ &= \sqrt{\frac{2\mathrm{p}!}{(\pi\,(p+|l|)!)}} \frac{1}{w(z)} \left(\frac{r\sqrt{2}}{w(z)}\right)^{|l|} \boldsymbol{L}_p^{|l|}\left(\frac{2r^2}{w^2(z)}\right) \\ &\quad e^{-\left(\frac{r^2}{w^2(z)}\right)} e^{-\left(\frac{ikr^2 z}{2R(z)}\right)} e^{\left(i(2p+|l|+1)\tan^{-1}\left(\frac{z}{z\boldsymbol{R}}\right)\right)} e^{(il\varphi)} \end{aligned} \tag{3}$$

Among them, l is the number of OAM modes, or called topological charges; p is the radial mode value, representing the phase change along the radial direction. $w(z) = \boldsymbol{w}_0\sqrt{1+\left(z/z\boldsymbol{R}\right)^2}$, w_0 is the beam radius of the Gaussian term, $zR = \pi w_0^2/\lambda$ represents the Rayleigh distance; $\boldsymbol{L}_p^{|l|}$ is a Laguerre polynomial. Since the beam carries the phase factor $e^{jl\varphi}$, its wavefront phase is no longer a continuous plane or spherical distribution, but has a spiral structure. Similarly, the Bessel beams also have a similar helical phase structure [50], the expression is:

$$\mathrm{BG}(r, \theta) = \boldsymbol{J}_l(\alpha r)\, e^{il\varphi} e^{-\left(\frac{r^2}{w^2}\right)} \tag{4}$$

where, α is the transverse wave number, l is the order of the Bessel function, and is also the number of OAM modes of the BG beam. Both LG beams and BG beams carrying different OAM mode numbers satisfy mutual orthogonality, so they have received extensive attention and research in the field of optical communication.

Inspired by the OAM mode in the optical frequency band B, reference [43] introduced OAM into the microwave frequency band and proposed the concept of electromagnetic vortex, and called the electromagnetic wave with OAM vortex electromagnetic wave. The energy of the conventional spherical electromagnetic wave radiates from the center to the outside. On the ring beam with the energy center as the origin, its phase is a fixed value, and the phase wavefront is a plane or a sphere. For the vortex electromagnetic wave, its energy is in the form of a ring. On the ring beam with the energy center as the origin, its phase is uniformly distributed. There is a phase gradient related to the topological charge between any two points on the ring, and its phase front is spiral. At the same time, the center point of the vortex electromagnetic wave perpendicular to the propagation axis has the characteristic of phase indetermination, also known as phase singularity, so the electric field intensity at the center of the vortex wave is zero. When the topological charge is 0, the phase and amplitude distributions present a plane wave or spherical wave distribution, and there is no spiral phase structure, and there is no phase singularity, as shown in Fig. 1.

III. ANTENNA DESIGN AND OAM EVALUATION

In this section, four different types of antennas are discussed, namely, active single microstrip patch antennas, travelling wave antennas, array antennas, and passive metasurface antennas. The OAM generating techniques are also described.

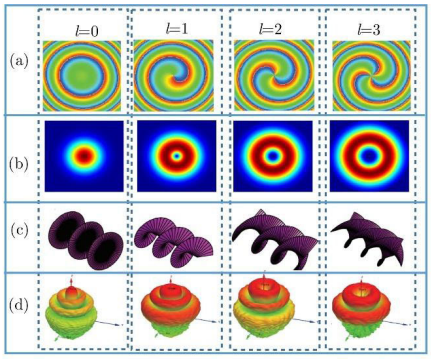

(a) Planar phase distributions (b) Planar amplitude distributions (c) Wavefront distributions (d) Radiating amplitudes spatial distributions

FIGURE 1. Radiation pattern of orbital angular momentum of different modes.

The special benefits and potential applications are also examined.

A. SINGLE MICROSTRIP PATCH ANTENNA

Because of its simple structure and easy implementation, the single microstrip patch antenna greatly reduces the production cost, so it has high research significance in generating orbital angular momentum in the radio frequency band. The OAM generated by a single microstrip patch antenna is mainly divided into two ways: the first is single-feed point input, by changing the antenna structure, the current can produce at least a 360° phase change on the antenna unit, thereby radiating vortex electromagnetic waves. The second type is double-feed point input, which can meet the conditions for generating vortex electromagnetic waves by changing the phase difference and amplitude of the antenna input current. Generally speaking, compared with multi-feed input antennas, single-feed input antennas have a simpler structure, are more convenient to operate, and have more obvious advantages in cost savings.

The OAM generated by feeding a single microstrip patch antenna through single feed point and double feed point can be divided into regular shape, irregular shape and ring nested structure according to the antenna structure. At present, for irregular shapes, the typical representative is the F-shaped structure using single feed point feed [51], as shown in Fig. 2(a), which gives the corresponding structural schematic diagram, physical diagram and simulation phase In the distribution diagram, multiple irregular F-shaped structures are combined to form an array and a phase shifter to generate vortex electromagnetic waves, but this structure has obvious disadvantages, and an additional phase shifter is needed to realize the phase change on each unit, so that greatly increases the production cost. For the single microstrip patch with a regular shape, the way to realize the OAM is simpler, and does not need to form an array and use an additional phase shifter, such as a regular elliptical structure [52] and regular octagonal structure [53], as shown in Fig. 2(b) and Fig. 2(c). Input current to the antenna through a single feed point to generate different resonant modes, thereby radiating corresponding with the method of generating vortex electromagnetic waves with irregular shapes, this form greatly reduces the production cost. However, the regular antenna structure shown in Fig. 2(b) and Fig. 2(c) can radiate two different modes of OAM by changing the position of the feed on the antenna structure. In the OAM mode, a simple one-to-two power division network [54] is proposed, as shown in Fig. 2(d). The circular microstrip patch antenna is fed with currents with equal amplitude and phase difference of 90° through the double feed point, and different degenerate modes are excited at different frequencies, and finally the antenna can simultaneously generate orbital angles of different modes at different frequencies. That is, the topological charge that can be generated at 1.62 GHz is 1, and the topological charge that can be generated at 2.73 GHz is 2, which solves the problem that there is only one topological charge for a structure, but due to different modes, the topological charges exist at the same frequency at the same time, which leads to the defect that the purity of the orbital angular momentum mode is not very high, so this also needs further research.

The above-mentioned typical irregular and regular single microstrip patch antennas can generate different modes of topological charges through single feed point and double feed point, but the ultimate research direction of vortex electromagnetic wave generation in the radio frequency band is to be able to different modes of topological charges are generated at frequency points, which can effectively increase the channel capacity of communication. Therefore, on the basis of the above-mentioned structures, scholars have achieved different topological charges at the same frequency by adopting single-feed point and double-feed point feed ring nested single microstrip patch antennas, as shown in Fig. 2(e). A ring nested structure with double-feed points is proposed in [55], and the relationship between the size of the ring structure and the feeding position is controlled, so that different modes of topological charges can be generated at the same frequency, but this structure is relatively more complicated, as each ring structure needs to adopt two feed points. In order to reduce the complexity of the structure, a ring nested structure with a single feed point is proposed [56], as shown in Fig. 2(f), each ring structure is fed separately, and finally the 4.65-5.20 GHz vortex electromagnetic waves with the topological charge mode numbers 2 and 3 can be generated simultaneously under the following conditions, but because this structure is nested with multiple rings, it can be seen from the measured phase distribution diagram in Fig. 2(f) that although this antenna structure has two different modes in a wide range at the same time, but the distance between the two ring structures is relatively close, and the isolation is not high, so the purity of the two modes is not very high, which also requires researchers to continue to do more exploration.

Reference [57] proposed a conical conformal loop patch antenna structure to generate vortex electromagnetic waves in different modes. As shown in Fig. 3, the loop antenna

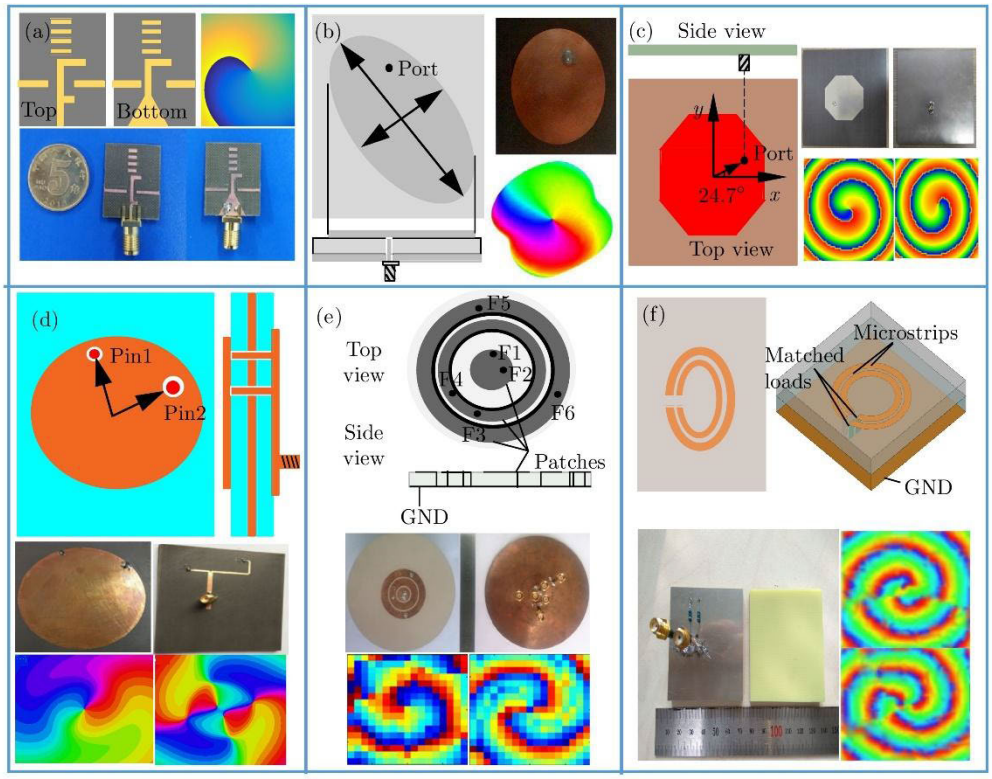

(a) F-shaped patch antenna[51] (b) Oval patch antenna[52] (c) Regular octagonal patch antenna[53]

(d) Circular patch antenna[54] (e) Two feed point annular nested patch antenna[55] (f) Single feed point annular nested patch antenna[56]

FIGURE 2. Illustration of single microstrip patch antenna designs and beam pattern.

(a) Configuration of the conical conformal patch antenna (b) Top view and bottom view (c) Measured intensity and phase distributions of l=1 vortex beam

FIGURE 3. Structure and radiation pattern of the conical antenna.

structure using a single feed point input retains the advantages of simple structure, by changing the feeding position, different modes of orbital angular momentum can be radiated at the same frequency point, digging out a rectangular groove on the ring structure can make the antenna radiate circularly polarized waves of different modes, and more importantly, the dielectric substrate shape of this conical conformal structure can improve the gain of the antenna. Finally, the reliability of the design is verified by comparing the experimental results with the simulation results. This structure is also produced by using a single microstrip patch antenna. A new technical approach to high gain, different modes of OAM.

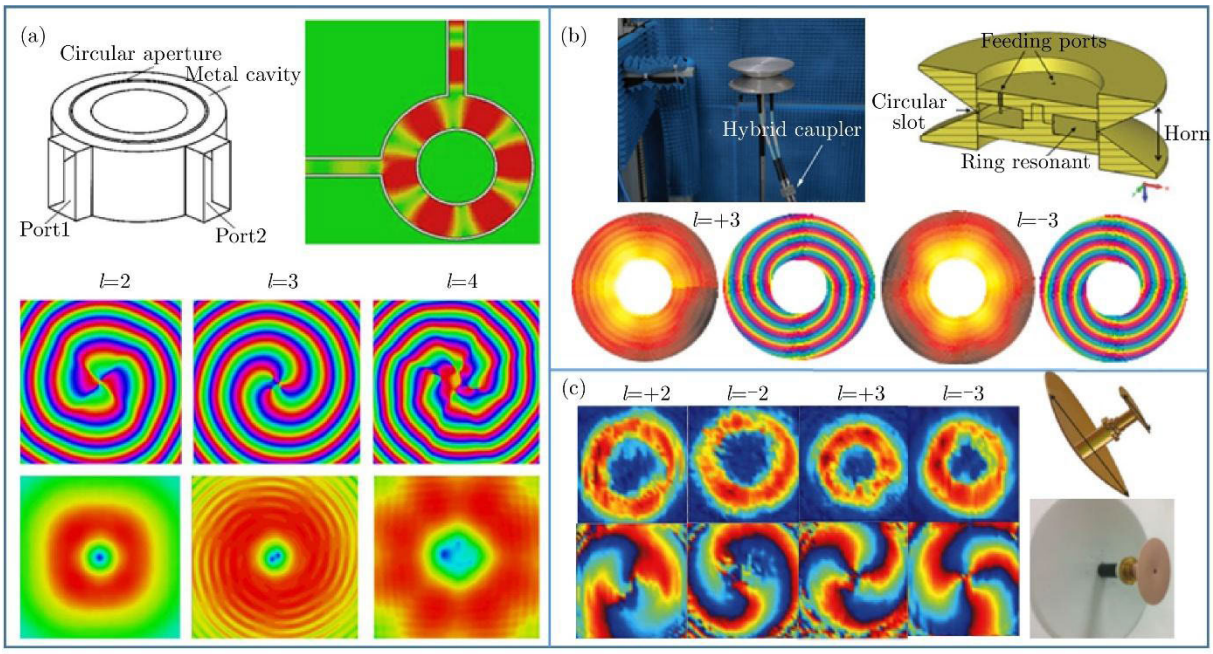

(a) Single ring[59] (b) Additional ring horn[60] (c) Double ring[61]

FIGURE 4. Structure and beam pattern of traveling wave antenna.

In the future, this structure can also be combined with the nested structure [58], which can generate high gain and carry multiple topological charges of different modes at the same frequency on the ring structure. Table 1 shows the main performance parameters corresponding to the vortex electromagnetic waves generated by the single microstrip patch antenna introduced above.

B. TRAVELING WAVE ANTENNA

Reference [59] proposed a circular traveling wave antenna to generate OAM waves. The 90° signal excites the traveling wave current distribution inside the metal annular cavity, and the generated electromagnetic wave radiates from the small annular groove at the top of the cavity, as shown in Fig. 4(a). Then, they add a circular horn structure is used to concentrate the energy radiation [60], as shown in Fig. 4(b). At the same time, in order to solve the problem of multiplexing between OAM modes in the radio frequency band, two annular metal cavities were deployed [61], as shown in Fig. 4(c), to realize the multiplexing of four OAM beams, while two reflectors are added to improve the gain and directivity of the antenna, reduce the OAM divergence angle, and make the vortex electromagnetic wave transmission distance longer.

The traveling wave antenna of this ring resonator can only generate one set of corresponding modes, and can only generate vortex waves in a narrow band range, which greatly limits the orthogonal multiplexing of OAM modes. In order to use orbital angular momentum to improve the spectrum utilization and imaging resolution of electromagnetic waves, how to generate vortex electromagnetic waves multiplexed with broadband multi-OAM modes has always been one of the focuses of researchers. The helical traveling wave antenna can be used to generate vortex electromagnetic waves with broadband multi-OAM modes due to its frequency-invariant characteristics and easy nesting characteristics, so it has attracted more attention.

Reference [62] used a single-arm Archimedes planar helical antenna to generate vortex electromagnetic waves in different OAM modes in different frequency bands, and used the principle of a circular current loop to theoretically deduce and prove that the Archimedes planar antenna generates vortex fields. The possibility has been verified by simulation and experiment respectively. The designed single-arm Archimedes planar helical antenna can generate vortex electromagnetic waves with OAM modes 1, 2 and 3 in the range of 1.30-3.25 GHz, 3.45-6.10 GHz and 6.25-10.50 GHz, respectively. The specific structure and experimental results is shown in Fig. 5(a). Reference [63] proposed a miniaturized nested three-dimensional helical antenna, as shown in Fig. 5(b), using a flexible dielectric material to load the helical antenna, and realizing double-loop nesting under the premise of ensuring a certain degree of isolation, which can be used in 4.80-5.20 GHz generates vortex electromagnetic waves with OAM mode numbers of 2 and 3, realizing multiplexing of OAM modes in the same frequency band. The four-arm equiangular planar helical antenna structure [64] as shown in Fig. 5(c) can realize the generation of vortex electromagnetic waves in four OAM modes within a certain bandwidth range.

TABLE 1. Comparison of various state-of-the-art single microstrip antennas performance.

Antenna type	Dimension (λ_0)	Operating frequency (GHz)	Gain (dBi)	OAM mode
Ref. [51]	1.02 × 1.25 × 0.06	17.00	-	+1
Ref. [52]	0.80 × 0.80 × 0.01	2.40	-	+1, +2
Ref. [53]	1.24 × 1.24 × 0.02	2.47	4.8	+1, -1
Ref. [54]	0.46 × 0.46 × 0.01	1.62	-	+1
Ref. [55]	0.46 × 0.46 × 0.02	2.73	-	+2
Ref. [56]	2.26 × 0.03 × 0.01	5.65	1.5, 1.8	+1, -2
Ref. [57]	1.00 × 1.00 × 0.13	4.65 to 5.20	6.6	+2, +3
Ref. [58]	1.00 × 0.01 × 0.01	2.00	-	+1

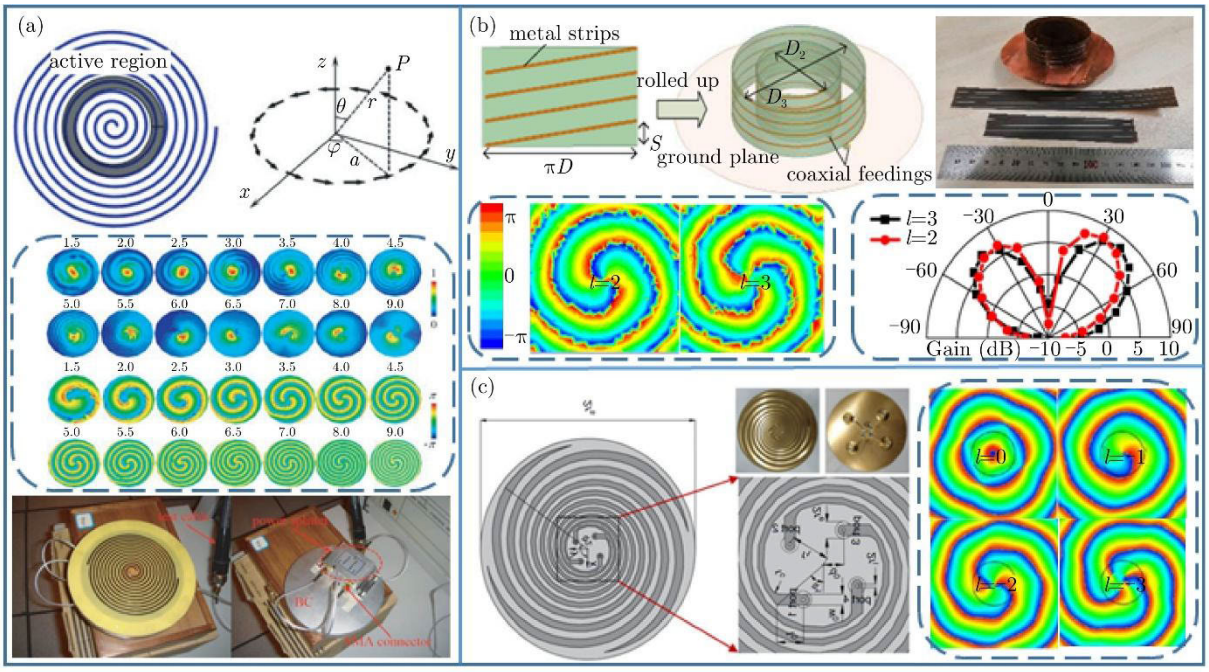

(a) Single-arm plane[62] (b) Stereo nesting[63] (c) Four-arm isometric angle[64]

FIGURE 5. Structure and beam pattern of helical traveling wave antenna.

Based on the above research, reference [65] proposed a dual-arm Archimedes spiral antenna based on dual feeds at the inner and outer arm ends, as shown in Fig. 6, which can generate vortex electromagnetic waves of different OAM modes, as well as different OAM modes at the same frequency point, realize the generation of opposite OAM modes by changing the internal and external feeding methods. Finally, the structure generates vortex electromagnetic waves with OAM mode numbers of ±1, ±2 and ±3 at frequencies of 3.00 GHz, 4.00 GHz and 4.80 GHz. At the same time, on this basis, the gain (6.70-10.00 dBi) and the divergence angle are reduced by adding a cavity, and the transmission distance of the vortex electromagnetic wave is increased, so that it is suitable for the OAM multiplexing communication system.

Reference [66] also proposed another three-dimensional spiral vortex electromagnetic wave antenna, the structure of which is shown in Fig. 7. Through theoretical analysis of the relationship between the number of modes and the helical size and wavelength, the vortex electromagnetic waves with OAM modes of 0, 1 and 2 were finally generated at three frequency points of 0.76 GHz, 1.55 GHz and 2.45 GHz. At the same time, in order to solve the problem that the single-arm spiral radiation field is uneven and the vortex wave mode is low, on the basis of the single-arm structure, a double-arm spiral with a symmetrical structure is also used to improve the radiation field. The electrical network simplifies the feeding structure of the double-armed helix. The team also reduced the height of the helix by loading a ring of metal sheets, and externally loaded cylindrical cavities to reduce back radiation. The dielectric plate on the top of the ring metal sheet can further increase the gain, so that the antenna has better directivity. This low-profile, high-gain and mode-tunable vortex electromagnetic wave antenna has broad application prospects in wireless communications.

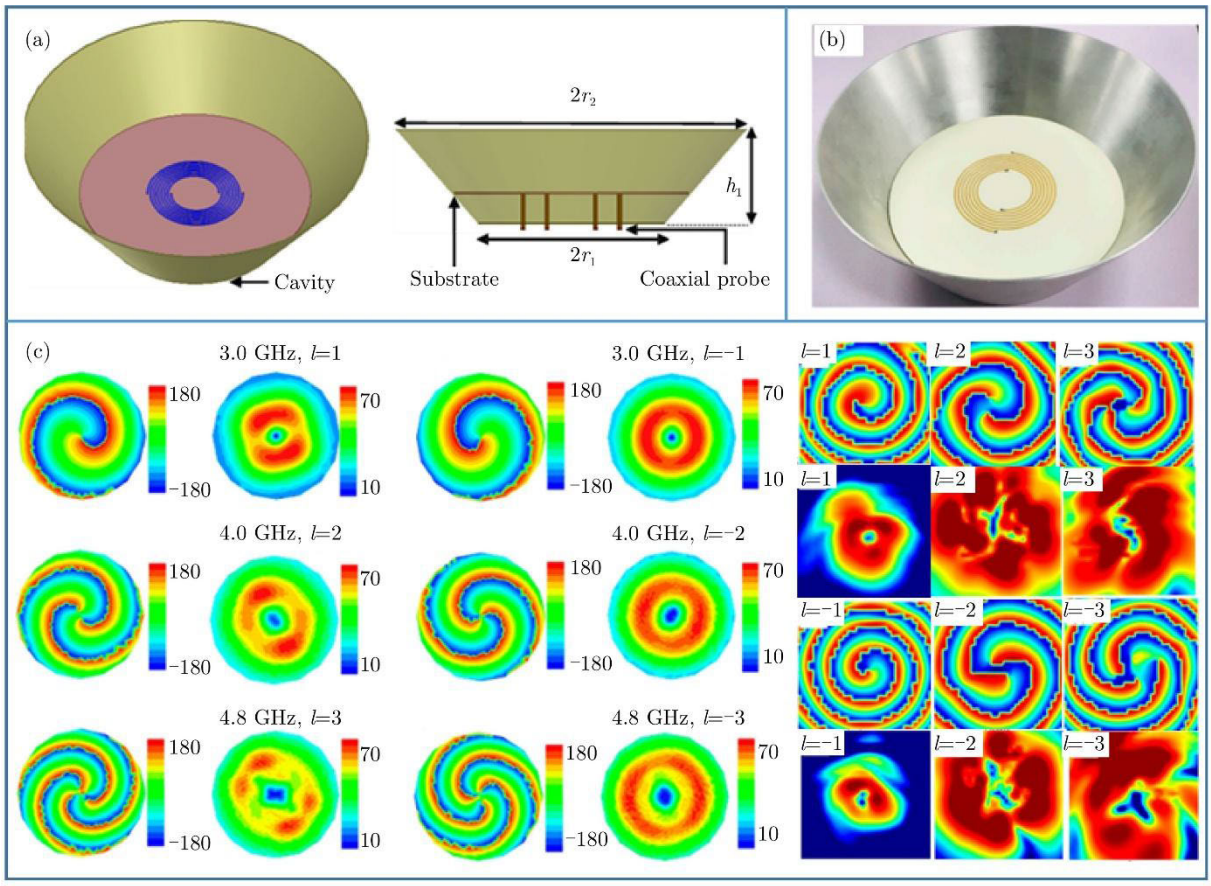

(a) Structure diagram (b) Physical map (c) Simulated and experimental results of phase and intensities distributions

FIGURE 6. Structure and beam pattern of Archimedes antenna [65].

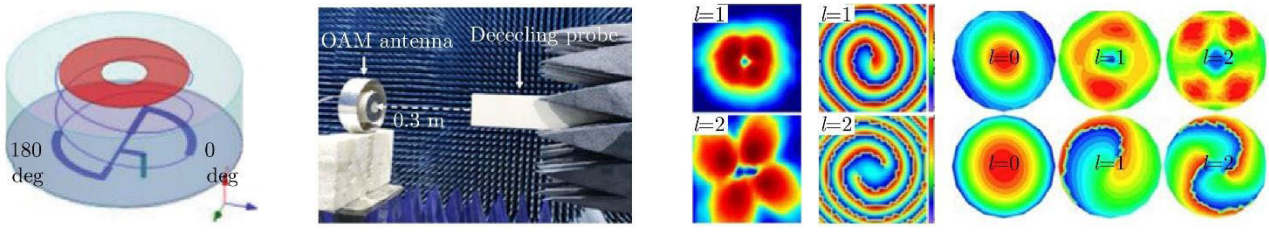

(a) Structure diagram (b) Experimental setup (c) Simulated and experimental results of phase and intensities distributions

FIGURE 7. Structure and beam pattern of 3D spiral vortex EM wave antenna [66].

According to the principle of vortex electromagnetic waves generated by the dual-arm planar helical antenna [67], [68], [69], in order to solve the problem of OAM multiplexing communication, reference [67] proposed a three-ring nested planar equiangular helix, as shown in Fig. 8, the microstrip feed network structure of the antenna is simple, and by adjusting the radius of the three nested rings. It can simultaneously generate OAM electromagnetic waves with mode numbers of 1, 3 and 5. At the same time, the metal reflector set between the helical structure and the feeding network can improve the radiation directivity and reduce the influence of radio frequency coaxial cables. The nested multi-arm helical antenna has great application potential in realizing multiplexing of multiple OAM modes. Table 2 shows the main

TABLE 2. Comparison of various state-of-the-art traveling wave antennas performance.

Antenna type	Dimension λ_0	Operating frequency (GHz)	Gain (dBi)	OAM mode
Ref. [59-61]	- Φ4.12 Φ20.00× 8.43	10.00 10.00 10.00	3.39 18.85 19.75	±3 ±2 ±3
Ref. [62]	Φ0.76× 0.01 Φ1.57× 0.02 Φ2.79× 0.08	1.30 to 3.25 3.45 to 6.10 6.25 to 10.50	-	1 2 3
Ref. [63]	>Φ0.90	4.80 to 5.20	7.60	2 3
Ref. [64]	Φ2.13× 0.03	5.60 to 6.00	-	0, -1, -2-, 3
Ref. [65]	2.60× 0.80 3.47× 1.07 4.16× 1.28	3.00 4.00 4.80	6.70 to 10.00	±1, ±2, ±3
Ref. [66]	Φ0.51× 0.13 Φ1.03× 0.26 Φ1.63× 0.41	0.76 1.55 2.45	4.55	0, 1, 2
Ref. [67]	Φ3.00× 0.57	3.00	6.94 6.76 5.49	1, 3, 5

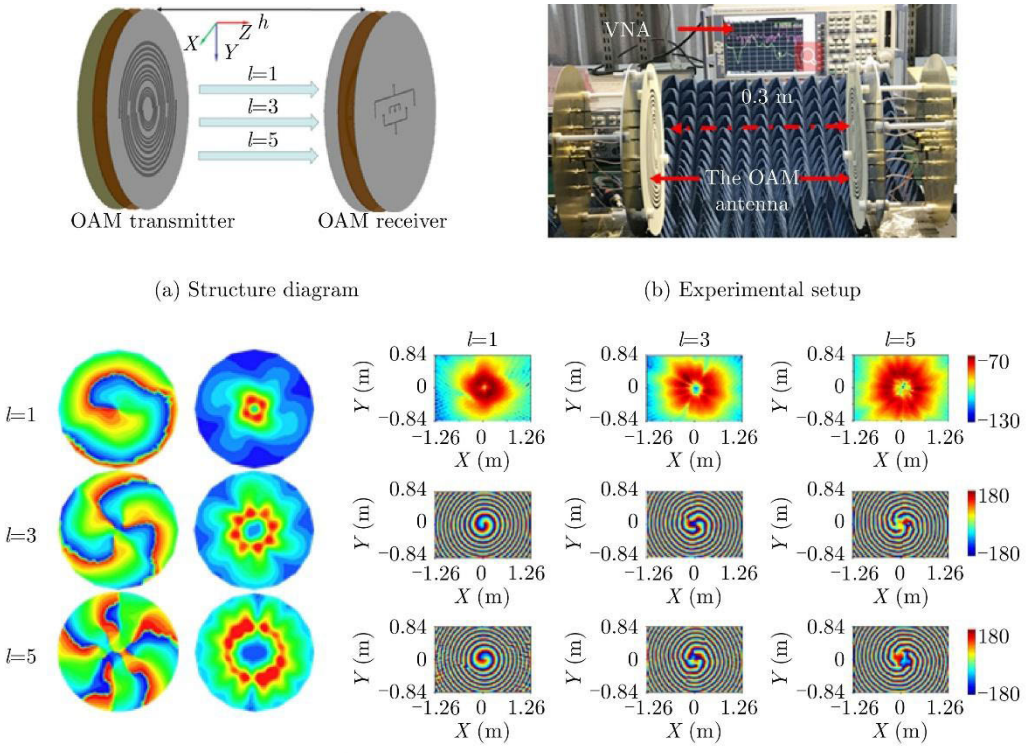

FIGURE 8. Structure and beam pattern of equi-angular helix [67].

performance parameters corresponding to the vortex electromagnetic waves generated by the traveling wave antenna introduced above.

C. ARRAY ANTENNA

The generation of vortex electromagnetic waves by array antennas is a relatively mature method at present. Compared with other antennas, the design principle of array antennas is simple and the structure is flexible. OAM electromagnetic waves of different modes can be generated by controlling the phase. At present, a variety of array antennas with different element structures have been proposed and used to generate OAM electromagnetic waves, such as dipole antenna arrays, microstrip patch antenna arrays, Vivaldi antenna arrays, and horn antenna arrays.

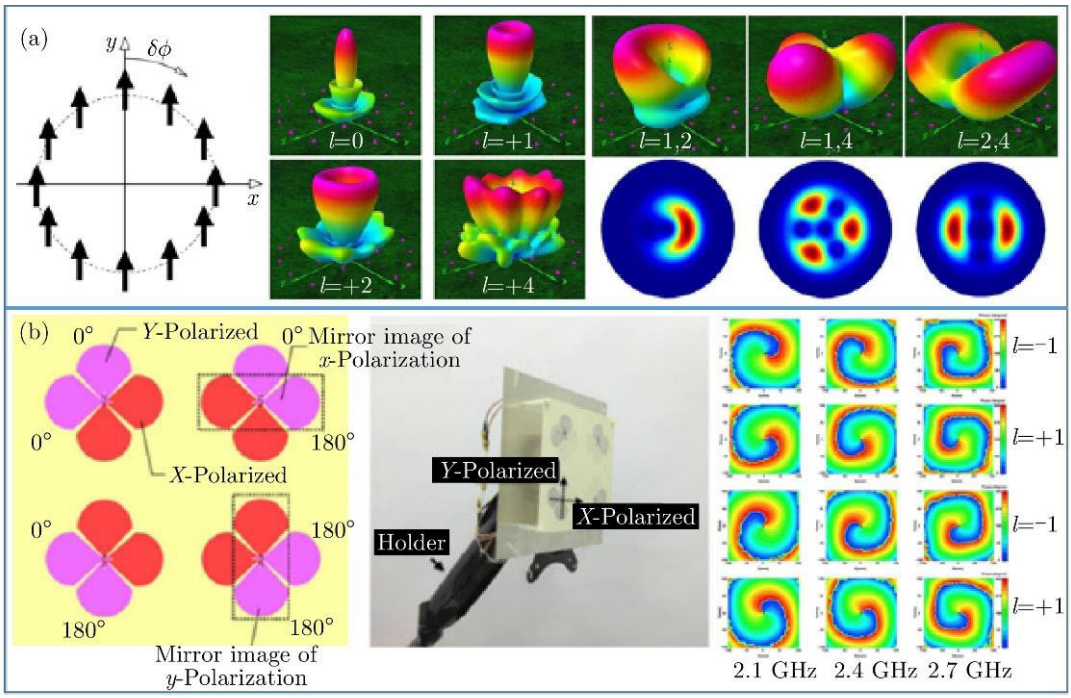

(a) Electrical dipole array antenna[43,70] (b) Wideband dual-polarized bow array antenna[71]

FIGURE 9. Electrical dipole and bow-array antenna.

1) DIPOLE ARRAY ANTENNA

Dipole antenna is the earliest, simplest and most widely used type of antenna. Reference [43] applied the theory of OAM to the low-frequency (<1.00 GHz) radio field for the first time, and designed a circular phased array with dipole antenna as the unit antennas to generate vortex electromagnetic waves. Reference [70] generate linearly polarized vortex electromagnetic waves with mode numbers 1 and 2, and systematically analyzed the directivity of antenna arrays, etc. The structure diagram and results are shown in Fig. 9(a). Reference [71] proposed an antenna array composed of a bow-tie dipole array element and a broadband phase-shifting feed network, which can generate circularly polarized OAM electromagnetic waves with a mode number of ± 1 at 2.10-2.70 GHz. The specific structure diagram and experimental architecture is shown in Fig. 9(b). The array provides four orthogonal channels for OAM communication, and the bit error rate is lower than 4.2×10^{-3}.

2) MICROSTRIP PATH ARRAY ANTENNA

Compared with the dipole antenna array, the elements of the microstrip patch antenna array are less affected by the mutual coupling effect, and it also has the advantages of low profile, simple structure, and low cost. Reference [72] proposed a phased array antenna composed of a rectangular microstrip patch array element and a microstrip phase-shifting feed network, as shown in Fig. 10(a). At 10 GHz, it is proved experimentally that vortex electromagnetic waves with $l = \pm 1$ can be generated. Since then, the microstrip patch antenna array has received extensive attention and research. Reference [73] designed a circular power divider structure with phase shifting function. The antenna structure is compact and easy to implement, which is suitable for radio communication and radar applications. Reference [74] used the patch array antenna for communication experiments for the first time, and generated OAM electromagnetic waves with mode numbers 0 and ± 1 at 5.75 GHz and carried out OAM multiplexing experiments. The experiment proved that OAM can not only improve communication capacity, but can also enhance the security of communication on the physical level. Reference [75] used the numerical control method to control the phase for the first time, and controlled the digital baseband signal through the FPGA device to realize the dynamic configuration of OAM in the radio frequency band. In [76], a circular array antenna with a multi-layer structure was used to realize the generation of dual OAM modes with low cross-coupling. Reference [77] proposed a low-profile microstrip rectangular array antenna, which excites quasi-cross-shaped apertures through U-shaped and M-shaped microstrip feeders to obtain two orthogonal polarizations, thereby realizing the generation of the specific results of different OAM modes are shown in Fig. 10(b). In order to generate multiple OAM modes with one array antenna, reference [78] proposed a wideband patch array antenna with reconfigurable polarization and OAM modes. Using an adjustable feed network composed of switching diodes, it can generate left-handed circular

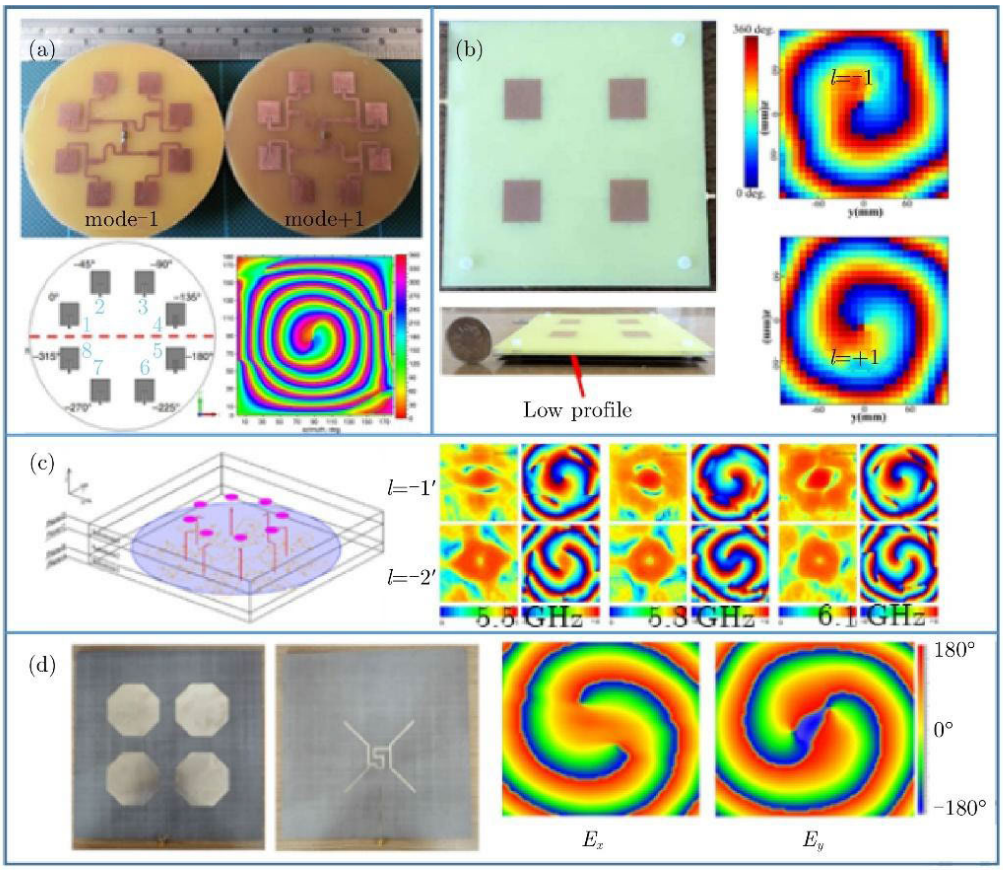

(a) Uniform circular array[72] (b) Low profile rectangular array[77] (c) Reconfigurable circular patch[79] (d) Octagon patch[53]

FIGURE 10. Structure and beam pattern of circular and rectangular patch antennas.

polarization in +1 mode and right-handed circular polarization in –1 mode. Reference [79] also used the switching diode electronic control method to realize the reconfigurable OAM mode, and generated OAM electromagnetic waves of ±1, ±2 and 0 at 5.50-6.10 GHz and 5.65-6.10 GHz. The specific results are shown in Fig. 10(c) shown. The octagonal patch antenna array [53] in Fig. 10(d) uses the high-order mode of the unit structure, breaks through the limitation of the number of array elements required to generate the OAM mode in the traditional situation, and only needs 4 patch units. The OAM electromagnetic wave with mode number -2 can be generated at 2.40 GHz. Reference [80] proposed a method to simplify the feed network. By introducing the optimal reference phase to reduce the number of required phases, only six phases are required to generate the number of modes in the frequency range of 2.33-2.73 GHz and OAM vortex electromagnetic waves of ±1, ±2, ±3. In addition, there are some antenna arrays that can achieve structure miniaturization [81], high gain [82], different polarization [83], different angles [84], high-order modes [85] and can be used for short distance communication [86] for OAM waves. Compared with other antenna arrays, the microstrip patch array antenna is easy to obtain OAM waves of different polarization forms, and the antenna profile is low, but the design of the feed network is more complicated, and it is difficult to simultaneously generate OAM electromagnetic waves of different modes, more detailed and in-depth research is needed for further optimization.

3) OTHER ARRAY ANTENNAS

In addition to the commonly used dipole and microstrip patch antenna arrays, researchers have also proposed a variety of antenna arrays with different array elements to generate OAM waves, such as Vivaldi antenna arrays, horn antenna arrays, resonant cavity antenna arrays, and single-arm helical antennas. It has the characteristics of broadband, high gain, and easy integration [87]. Fig. 11(a) shows a compact broadband Vivaldi antenna array [88], in which eight Vivaldi antenna elements are folded sequentially to form a hollow cylinder, which can generate a vortex with a mode number of 0, ±2 at 2.70-2.90 GHz rotating electromagnetic waves. The horn antenna has good radiation directivity and high gain, so it is often used as an array antenna unit. The circular horn antenna array in Fig. 11(b) [89] can achieve zero mode number in

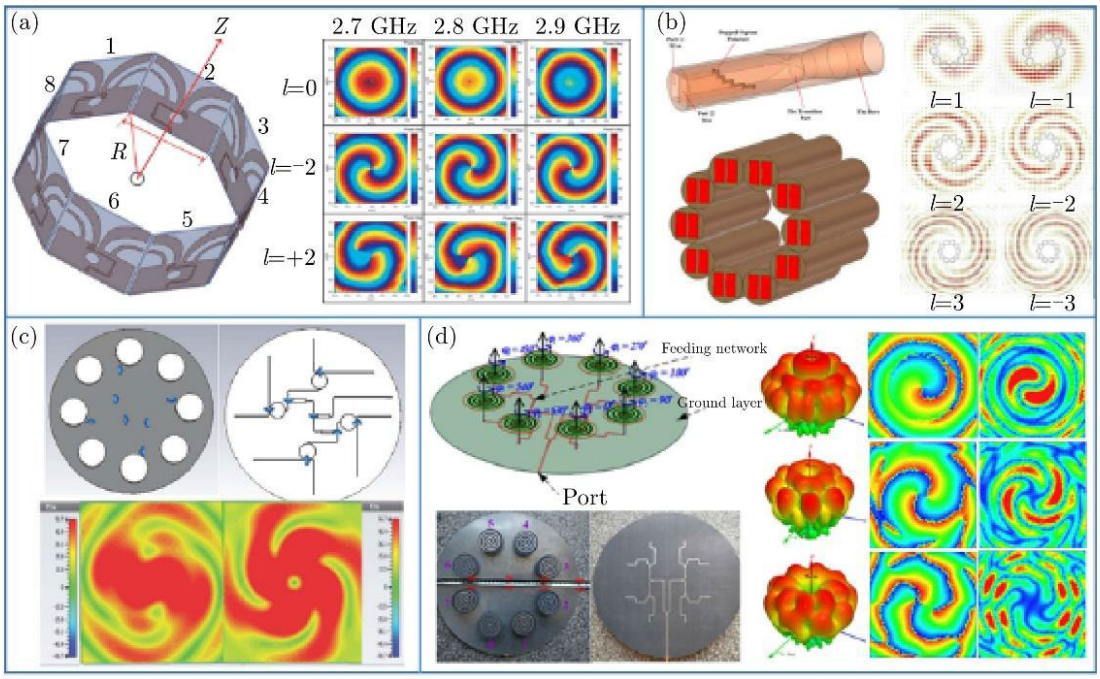

(a) Vivaldi antenna[88] (b) Horn antenna[89] (c) Dielectric resonator antenna[93] (d) Single-arm helical antenna[95]

FIGURE 11. Structure and beam patterns of various types of array antennas.

three polarization states, ±1, ±2, ±3, ±4 OAM electromagnetic waves. Reference [90] uses a circular horn antenna array in the X-band to generate high-order OAM electromagnetic waves, which can be used for vortex electromagnetic wave radar imaging. Reference [91] proposed water immersed circular horn antenna array can generate vortex electromagnetic waves with mode numbers 0, 1, 2, and 3 in pure water, which is conducive to improving the resolution of underwater microwave imaging systems. Reference [92] uses the Rotman structure to analyze the three array of element horn antennas is fed to generate multi-mode OAM. The cylindrical dielectric resonator antenna array shown in Fig. 11(c) [93], by correctly selecting the dielectric constant and height of the substrate, the loss of the transmission line and the generation of surface waves can be avoided. Reference [94] proposed a new design for multi-mode OAM using surface plasmons, which can simplify the generation of vortex beams. In addition, the single-arm Archimedes planar helical antenna array proposed in [95] can add phases to antenna elements through mechanical rotation and microstrip feed network, and can operate at 3.40-3.90 GHz, 3.40-4.10 GHz and 3.90-4.70 GHz, respectively. Vortex electromagnetic waves with OAM modes 1, 2 and 3 are generated in the frequency range of GHz, as shown in Fig. 11(d). Compared with dipole antenna arrays and microstrip patch antenna arrays, antenna arrays with other structures have unique advantages and development prospects. In the future, more antenna arrays with unique structures will be proposed to be suitable for wireless communication, radar imaging, remote sensing detection and other different directions. Table 3 lists the OAM waves and their performances generated by some currently proposed array antennas.

D. METASURFACE ANTENNA

The use of phased array antennas to generate OAM waves requires a complex feed network, which still has great limitations in practical applications. Therefore, in recent years, the use of electromagnetic metasurface technology to generate OAM waves has been proposed, and has received extensive attention from many researchers in the radio frequency band. A metasurface is an ultrathin 2-dimensional array surface composed of metamaterial resonant units periodically arranged in subwavelength sizes. It can realize sudden changes in the amplitude or phase of electromagnetic waves by changing the shape and size of the resonant units [96]. Compared with traditional phased array antennas, metasurface antennas have the advantages of low profile, simple feeding system, and easy beamforming [97]. The metasurface antennas currently used to generate OAM waves can be divided into four categories: reflective metasurfaces, transmissive metasurfaces, holographic metasurfaces, and digitally encoded metasurfaces. Among them, reflective metasurfaces and digitally coded metasurfaces are favored by researchers due to their advantages such as simple structure and process and diversified regulation.

TABLE 3. Comparison of various state-of-the-art traveling wave antennas performance.

Array element structure	Antenna type	Dimension λ_0	Operating frequency (GHz)	Gain (dBi)	OAM mode
Microstrip patch	Ref. [72]	Φ2.00× 0.05	10.00	2.45	±1
	Ref. [73]	Φ0.91× 0.69 × 0.01	2.50	-	$+1$
	Ref. [74]	Φ1.61× 0.01	5.75	8.35	$0, \pm1$
	Ref. [83]	1.67 × 1.671 × 0.10	4.80	9.00	±1
	Ref. [75]	2.03 × 2.03 × 0.01	1.90	-	$0, \pm1, \pm2, \pm3$
	Ref. [76]	Φ4.84× 0.03	5.72 to 5.95	-	±1
	Ref. [86]	Φ6.00	8.00 to 12.00	-	$0, +1, +2, +3$
	Ref. [68, 77, 80, 82, 84]	2.20 × 2.00 × 0.10 3.10 × 3.10 × 0.07 0.61 × 0.61 × 0.02 Φ3.33× 0.06 Φ1.90× 0.06	5.40 to 5.60 9.70 to 10.70 2.40 2.33 to 2.73 5.80	7.35 8.05 14.15 9.55 9.25 8.95 - 6.35 >6.55	-1 $+1$ 0 ±1 ±2 ±3 $-1, -2$ $\pm1, \pm2, \pm3$ $0, -1, -2, -3$
	Ref. [78]	1.28× 1.28 × 0.07	2.50	3.15 3.05	$+1$ -1
	Ref. [79]	Φ5.60× 0.05	5.50 to 6.10 5.65 to 6.10	9.15 4.05 7.45	±1 ±2 0
	Ref. [33]	4.85 × 4.85 × 0.14	13.50 to 16.70	-	$-1, -2$
	Ref. [85]	7.50 × 7.50	18.00	-	$+5$
	Ref. [81]	Φ1.00× 0.02	1.55	-	$\pm1, +2$
Trumpet	Ref. [89]	Φ4.00	2.20	8.75	$0, \pm1, \pm2, \pm3, \pm4$
	Ref. [90]	Φ10.00	9.90	-	$0, +1, +2, +3, +4, +5, +6, +7$
	Ref. [92]	8.86 × 9.06 × 0.02	9.70	8.48	$0, \pm1$
	Ref. [91]	Φ0.80× 0.34	2.45	-	$0, +1, +2, +3$
Dipole	Ref. [43, 70]	Φ4.00 Φ1.50	1.00 2.40	-	$+1, +2, +4$ $+1, +2$
	Ref. [71]	1.76× 1.76 × 0.01	2.10 to 2.70	-	±1
Vivaldi	Ref. [87]	Φ1.57× 1.20	6.00	7.00	$0, \pm1, \pm2, \pm3, +4$
	Ref. [88]	Φ0.51× 0.40	2.70 to 2.90	-	$0, \pm2$
Resonant cavity	Ref. [93]	Φ1.00× 0.16	3.50	-	$+1, \pm2$
Surface plasmons	Ref. [94]	Φ3.20× 0.06	5.50 5.80 6.00 6.30 6.60	-	-2 -1 0 $+1$ $+2$
Single arm spiral	Ref. [95]	Φ5.33× 0.47	3.40 to 4.70	8.50	$+1, +2, +3$

References [98], [99], and [100] used the reflective metasurfaces of rectangular patch unit, dipole unit and "cross-shaped" patch unit [100] respectively to achieve a single OAM wave, angle separation generation of OAM wave and polarization separation OAM wave, and the corresponding simulation and experimental verification are carried out, as shown in Fig. 12(a) and Fig. 12(b). Reference [101] realized the generation of mixed-mode OAM waves, and performed efficient reception and mode separation of the generated OAM waves. Subsequently, reference [102] continued to study the generation of OAM waves with different polarizations (linear polarization, left-handed circular polarization, and right-handed circular polarization), as shown in Fig. 12(c). In the direction of polarization, OAM waves with a mode of ±1 and broadband (9-11 GHz) OAM waves have been generated in two bands (C-band and X-band) [103], [104]. In the past two years, the use of reflective metasurface antennas to generate OAM waves has sparked an upsurge. Reference [105] used a double-layer reflector structure to realize OAM modes with low divergence angles, and the generated OAM waves can be transmitted over long distances ($46.9\lambda_0$), like Fig. 12(d). Reference [106] realized the generation of reconfigurable OAM waves with mode numbers $l = -1, 0, 1$ through

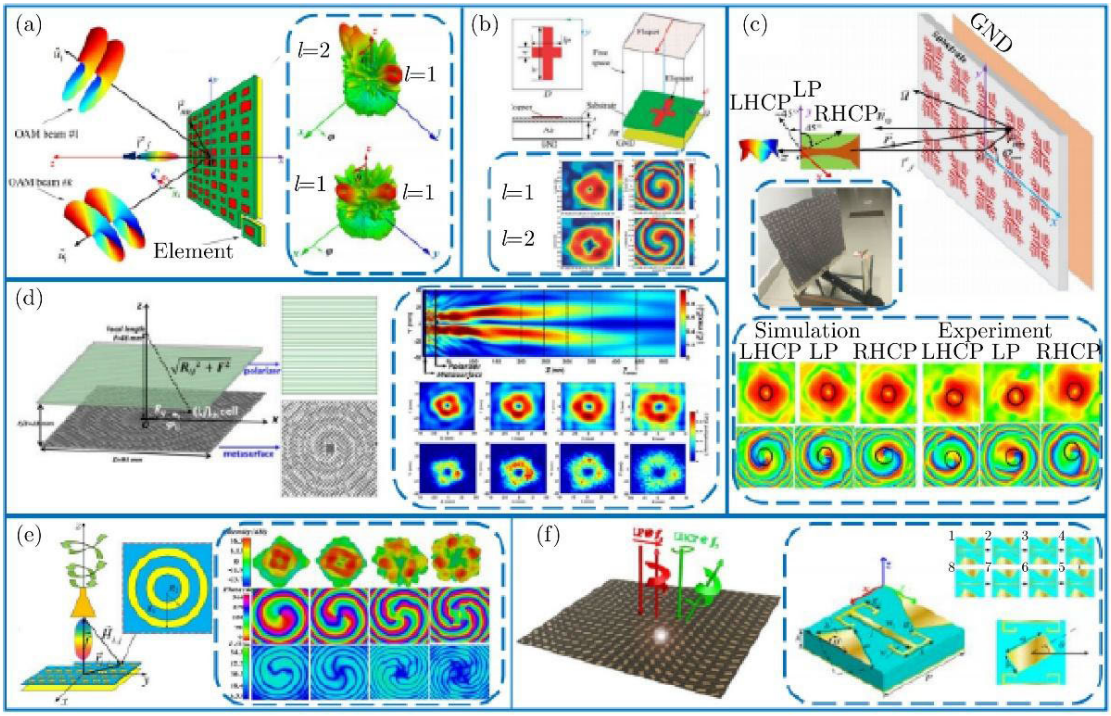

(a) Angular-separated OAM waves[99] (b) Polarization-separated OAM waves[100] (c) Multi-polarization OAM waves[102]

(d) Double-layer reflector plate realizes low-divergence OAM waves[105] (e) Miniaturization structure generates OAM waves[111] (f) Dual-band OAM waves[112]

FIGURE 12. Illustration of OAM radiation generated by metasurface antennas.

an adjustable phase-shifted feed network. Reference [107] used the Pancharatnam-Berry phase to generate broadband OAM waves, and realized the generation of vortex electromagnetic waves with a bandwidth ranging from 6.95 to 18.00 GHz. In addition, many researchers also pay attention to the generation of vortex waves in multi-mode and higher-order modes [108], [109], [110], by adjusting the size parameters of the structure, a phase coverage of 2π can be achieved, and then different OAM modes can be realized. Reference [111] used the miniaturized reflective metasurface antenna to realize the generation of OAM waves in different modes, as shown in Fig. 12(e), using the double-ring structure as the resonant unit ($0.38\lambda_0 \times 0.38\lambda_0$), greatly reducing the overall size of the array. In [112], the Pancharatnam-Berry phase and the resonant phase were used to generate different modes of OAM waves in different bands under the same planar structure, as shown in size of the font structure produces OAM waves of modes 1 and 2 at 5.20 GHz and 10.50-12.00 GHz, respectively.

Reference [113] used the concept of high-order phases and an adjustable phase network structure composed of diodes to realize the generation of reconfigurable OAM waves, as shown in Fig. 13. Compared with the above-mentioned metasurface structure, this metasurface can realize ± 1, ± 2, ± 3 order OAM modes, which greatly improves the utilization efficiency of the structure. Moreover, the generated OAM waves of different modes all work at the same frequency, which also facilitates the application of the OAM multiplexing technology in the communication system. In addition, the structure can also realize the scanning ($-55°-55°$) and focusing of the electromagnetic beam, which broadens the application range of the antenna. The reflective metasurface has a simple structure and diverse functions, and is an important research direction for metasurface antennas to generate OAM waves. At present, the generation of vortex waves by reflective metasurfaces still has great limitations. In the future, scholars can focus on reconfigurable modes, angles for further research in several aspects such as multiplexing and broadband.

While reflective metasurfaces are widely used, transmissive metasurfaces are gradually coming into people's field of vision. Reference [114] used the transmission metasurface to generate the OAM wave with mode 2, as shown in Fig. 14(a), the left-handed circularly polarized plane wave forms a right-handed wave after passing through the metasurface. In recent years, transmissive metasurfaces have also received extensive attention. Reference [115] effectively reduced the divergence angle of the vortex wave by using

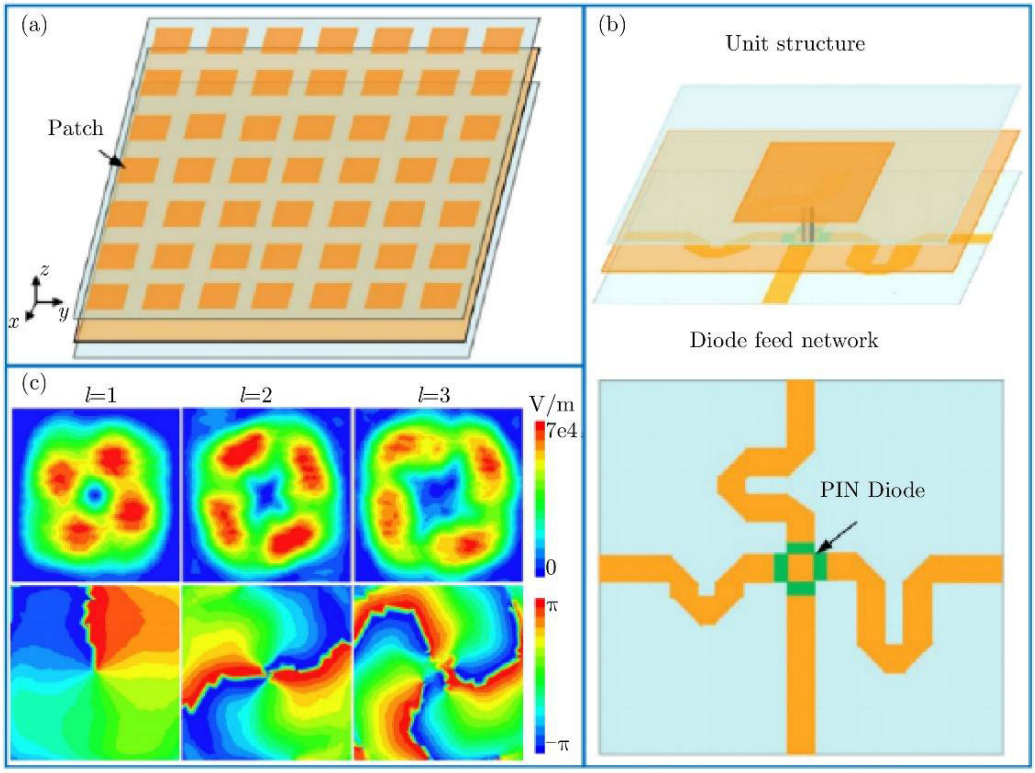

(a) Configuration of antenna structure (b) Unit structure diagram (c) Intensity and phase distribution diagram

FIGURE 13. Structure and phase diagram of adjustable antenna.

the amplitude-phase dual control method. In [116], the generation of OAM waves with a divergence angle of 9° and a mode of $l = 1$ was realized through the structural unit of 4 layers of metal and 3 layers of dielectric. Reference [117] generated OAM waves with modes 0 and 1 under different polarizations, as shown in Fig. 14(b). Reference [118] used a metasurface lens to achieve the convergence of OAM waves, reducing the divergence angle from 50° to 22°. In [119] and [120], by adjusting the unit size of the metasurface, the generation of polarization conversion and angle-separated OAM waves is realized respectively. As shown in Fig. 14(c), the modes $l = -2, -1, 0, 1, 2$ OAM waves. In [121], a 13-layer cell structure combined with a PIN diode was used to realize a mode-reconfigurable vortex wave. In [122], the single-layer ultra-thin ($0.05\lambda_0$) structure was used to generate vortex waves in modes 1 and 2, respectively. In addition, there are OAM waves generated by miniaturization [123], [124] and single-layer structure [125], and OAM waves that achieve polarization separation by using all-dielectric metasurfaces in [126], as shown in Fig. 14(d). It is shown that OAM waves with modes –1 and 2 are generated under TE and TM incident waves, respectively. Compared with the reflective metasurface, the OAM wave generated by the transmissive metasurface is not easily affected by the incident wave, and the mode purity is higher, but the structure of the transmissive metasurface is more complex, usually requiring a multi-layer structure, which increases the difficulty of the process, and Radiation gain is low, which also requires further research.

In addition to the traditional reflective and transmissive metasurfaces, references [127], [128], and [129] proposed the use of a new structure called a holographic metasurface to generate OAM waves, as shown in Fig. 15. In Fig. 15(a), the OAM waves with modes –1 and 1 are generated at different angles. In Fig. 15(b), the OAM waves with topological charges of 2 and 4 were generated by using different arrangements of structural units. The holographic metasurface combines the holographic algorithm with the metasurface to achieve more precise beam control. The generated OAM wave mode has high purity and small divergence angle, and can realize the adjustment of the OAM wave angle. The disadvantage is that the algorithm is more complicated and the amount of calculation is large, so far there are few studies.

In addition, references [130], [131], [132], [133], and [134] proposed a new digitally coded metasurface to generate OAM waves. They realized a reconfigurable and angle-separated and mode-separated OAM waves, as shown in Fig. 16. At the same time, reference [135] realized multi-mode OAM beam radiation by using digital coding Pancharatnam-Berry phase, polarization separation digital coding [136] and full space digital coding [137]. Compared with the traditional

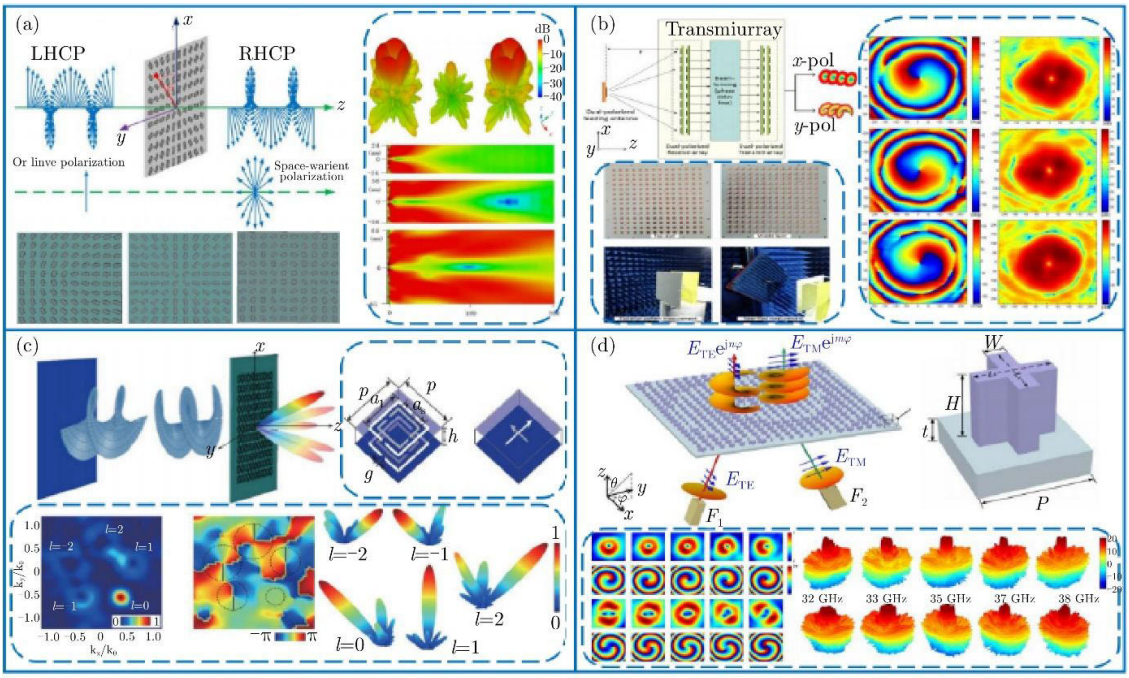

(a) Polarization-converted OAM waves[114] (b) Polarization-separated OAM waves[117] (c) Angled-separated OAM waves[120] (d) All-dielectric metasurface[126]

FIGURE 14. Structure and polarization of transmit antenna array.

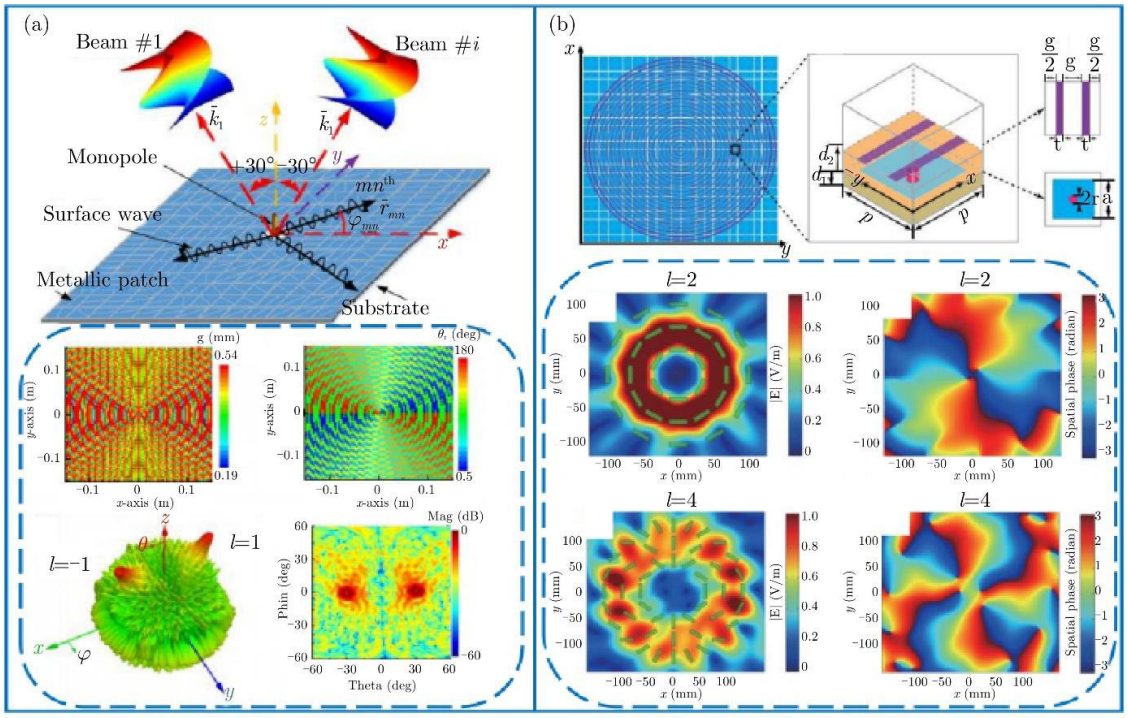

(a) Angle-separated OAM waves[128] (b) OAM waves of two different modes[127]

FIGURE 15. Structure and beam patterns of holographic metasurface.

metasurface, the phase of the digitally coded metasurface unit is composed of a limited number of binary values, which greatly simplifies the computational complexity. At the same time, the generated vortex wave still maintains a good helical

TABLE 4. Comparison of various state-of-the-art metasurface antennas performance.

Antenna structure	Antenna type	Dimension λ_0	Operating frequency (GHz)	Gain (dBi)	OAM mode
Reflective metasurface	Ref. [98-104]	10.00× 10.00 × 0.12	5.80	-	1, 2,4
		10.00 × 10.00 × 0.12	5.80	-	x-polarization 1,y-polarization 2 1,1;1,2
		10.00 × 10.00 × 0.07	5.50 to 6.50	-	1, 2
		10.00 × 10.00 × 0.07	5.80	-	1
		12.60 × 12.60 × 0.22	10.00	-	1,-1(±30°)
		8.82 × 8.82 × 0.16	6.00	17.7	1,-1(±30°)
		14.70 × 14.70 × 0.26	10.00	19.8	1
		10.50 × 10.50 × 0.16	9.00 to 11.00	19.9	
	Ref. [107]	6.72 × 6.72 × 0.13	6.95 to 18.00	-	1; 2
	Ref. [108]	Φ7.00 × 0.10	10.00	10	0; 1; 2
	Ref. [105]	12.50 × 12.50 × 3.00	40.25	-	−1
	Ref. [106]	2.38 × 2.38 × 0.07	5.00 to 6.30	11.05	−1,0,1
	Ref. [109]	Φ6.46 × 0.15	18.00 to 42.00	-	1,3
Transmission metasurface	Ref. [110]	Φ15.00 × 0.10	5.00 to 7.50	17.93	4
	Ref. [111]	3.87 × 3.87 × 0.11	5.80	15.4	1;2;3;4
	Ref. [112]	8.50 × 8.50 × 0.10 4.20 × 4.20 × 0.05	5.20	-	1 2
	Ref. [113]	3.50 × 3.50 × 0.10	300.00	>20	−1, −2, −3,1,2,3
	Ref. [114]	5.00 × 5.00 × 0.08	11.80	-	2
	Ref. [119, 120]	9.60 × 9.60 × 0.05 4.58 × 4.58 × 0.05	17.85 17.85	- -	2;4 −1, −2,0,1,2
	Ref. [121]	6.90 × 7.30 × 2.60	10.00	-	−1, −2, −3, −4,1,2,3,4
	Ref. [126]	9.40 × 9.40 × 0.76	32.90 to 36.80	15	x-polarization −1, y-polarization 2
	Ref. [115-118]	18.60 × 18.60 × 0.66 4.67 × 4.67 × 0.15 9.20 × 9.20 × 0.23 4.80 × 4.80 × 0.20	10.00 10.00 13.00 to 15.00 9.60 to 10.32	- 14.5 26, 20 -	2 1 x-polarization 0, y-polarization 1 1;2;3
	Ref. [122]	6.00 × 6.00 × 0.05	10.00	-	1;2
	Ref. [123]	8.00 × 8.00 × 0.15	10.00 to 11.30	-	1
	Ref. [124]	4.88 × 4.88 × 0.14	14.00	-	1
	Ref. [125]	5.25 × 5.25 × 0.10	10.00	10.85	2
Holographic metasurface	Ref. [127]	3.50 × 3.50 × 0.10	6.20	-	2;4
	Ref. [128-129]	20.20 × 20.20 × 0.11 20.20 × 20.20 × 0.11	20.00 20.00	- -	−1, 1(±30°) 1;2;3

TABLE 4. *(Continued.)* **Comparison of various state-of-the-art metasurface antennas performance.**

Digitally encoded metasurface	Ref. [130-131]	6.30 × 6.30 × 0.04	4.75	-	1,2
		6.67 × 6.67 × 0.04	5.00	-	1(0°,30°) 2(0°,20°)
	Ref. [132-134]	9.00 × 9.00 × 0.06	6.00	-	1
		8.84 × 8.84 × 0.08	8.50	-	x-polarization -2, 2 y-polarization -1, 1
		5.85 × 5.85 × 0.07	7.10 to 7.50 7.00 to 7.50	14.7 11.1	-1 1
	Ref. [135-137]	12.00 × 12.00 × 0.10	14.50 to 15.50	-	1(±30°)
		Φ15.00 × 0.15	15.00	-	x-polarization 1 y-polarization -1
		4.80 × 4.80 × 0.05	10.00	-	1, -1

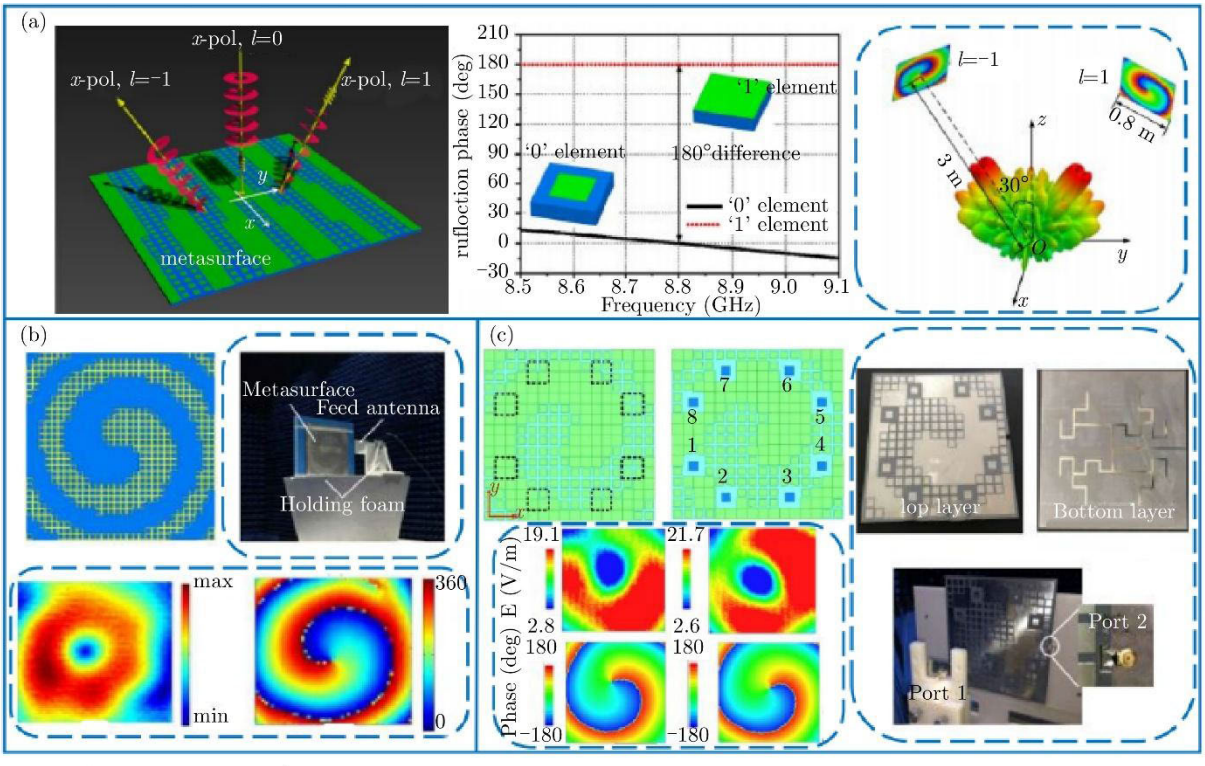

(a) Polarization-separated OAM waves[132] (b) OAM waves with mode 1[133] (c) Simultaneously generating OAM waves with two modes[134]

FIGURE 16. Structure and beam patterns of digitally encoded metasurfaces.

phase characteristic, and also making it valuable for research. This new type of metasurface antenna may play an important role in the generation of OAM waves in the future. Table 4 lists some currently reported metasurface antennas for generating OAM waves and their properties.

IV. CONCLUSION

The vortex electromagnetic wave carrying OAM has great potential application value in the field of wireless communication, radar detection and imaging, but the generation method of vortex electromagnetic wave is not optimal,

especially the broadband and multi-OAM mode antenna design still faces great challenges.

This paper mainly reviews and summarizes the progress of antenna structures that generate vortex electromagnetic waves in the radio frequency spectrum. The origin, development history and application trend of vortex electromagnetic waves are briefly introduced. The research progress of vortex electromagnetic wave generation technology by antennas, the advantages and disadvantages of each type of vortex antennas are summarized and compared, and then the future development is summarized and prospected on the basis of these four types of antennas.

There are still some issues that require resolution. For instance, many OAM multiplexing studies continue to employ pricey and bulky components that are unsuitable for widespread usage and practical implementation. It is difficult to produce and detect highorder and multi-mode OAM beams with a finite-size aperture. The development of system components like transmitters, multiplexers, demultiplexers, and receivers is crucial to the future viability of OAM. These elements must offer size and cost savings and be compatible with current technology. Moreover, the propagation channel's condition has a significant influence on OAM-based connections, and issues that arise in some challenging and complicated channel circumstances must be addressed and resolved. In future research, how to design and manufacture a vortex antenna with a simpler structure and lower cost, while also being able to generate broadband, multi-OAM modes, and high-quality vortex electromagnetic waves, will be the unremitting efforts of the academic community. Moreover, the multiplexing between different modes of vortex electromagnetic waves and the demultiplexing of composite vortex electromagnetic waves will also be the focus of future research. The analysis and research on the transmission characteristics of vortex electromagnetic waves in different dispersion systems will also be the key to the scientific problems that have to be faced in the application field. The progress and maturity of vortex electromagnetic wave related technologies will promote its increasingly important role in wireless communication systems, vortex radar imaging systems, and medical imaging systems.

REFERENCES

[1] Q. Mai, C. Wang, X. Wang, S. Cheng, M. Cheng, Y. He, J. Xiao, H. Ye, D. Fan, Y. Li, and S. Chen, "Metasurface based optical orbital angular momentum multiplexing for 100 GHz radio over fiber communication," *J. Lightw. Technol.*, vol. 39, no. 19, pp. 6159–6166, Oct. 15, 2021.

[2] L. Zhang, J. Guo, and T. Ding, "Ultrathin dual-mode vortex beam generator based on anisotropic coding metasurface," *Sci. Rep.*, vol. 11, no. 1, pp. 1–9, Mar. 2021.

[3] O. Emile and J. Emile, "Energy, linear momentum, and angular momentum of light: What do we measure," *Annalen der Physik*, vol. 530, no. 12, pp. 1081–1097, 2018.

[4] S. Yoshida, C. McGibboney, and T. Sasaki, "Nondestructive evaluation of solids based on deformation wave theory," *Appl. Sci.*, vol. 10, no. 16, pp. 1–23, 2020.

[5] M. Cosic, S. Petrovic, and N. Neskovic, "Quantum rainbows in positron transmission through carbon nanotubes," *Atoms*, vol. 7, no. 1, pp. 1–18, 2019.

[6] A. Soluyanov and D. Vanderbilt, "Wannier representation of $\mathbb{Z}_2$ topological insulators," *Phys. Rev. B, Condens. Matter*, vol. 83, no. 3, pp. 108–119, 2011.

[7] D. A. Abanin, T. Kitagawa, I. Bloch, and E. Demler, "Interferometric approach to measuring band topology in 2D optical lattices," *Phys. Rev. Lett.*, vol. 110, no. 16, pp. 1653–1661, Apr. 2013.

[8] M. V. Berry, "Optical vortices evolving from helicoidal integer and fractional phase steps," *J. Opt. A, Pure Appl. Opt.*, vol. 6, no. 2, pp. 259–268, Jan. 2004.

[9] J. Yang, C. Qian, X. Xie, K. Peng, S. Wu, F. Song, S. Sun, J. Dang, Y. Yu, S. Shi, J. He, M. J. Steer, I. G. Thayne, B.-B. Li, F. Bo, Y.-F. Xiao, Z. Zuo, K. Jin, C. Gu, and X. Xu, "Diabolical points in coupled active cavities with quantum emitters," *Light, Sci. Appl.*, vol. 9, no. 1, pp. 1–8, Jan. 2020.

[10] M. V. Berry, "Quantal phase factors accompanying adiabatic changes," *Proc. Roy. Soc. London*, vol. 392, no. 1802, pp. 45–57, 1984.

[11] V. Kotlyar, E. Abramochkin, A. Kovalev, and A. Savelyeva, "Product of two Laguerre–Gaussian beams," *Photonics*, vol. 9, no. 7, pp. 1–14, 2022.

[12] M. Q. Mehmood, S. Mei, S. Hussain, K. Huang, S. Y. Siew, L. Zhang, T. Zhang, X. Ling, H. Liu, J. Teng, A. Danner, S. Zhang, and C.-W. Qiu, "Visible-frequency metasurface for structuring and spatially multiplexing optical vortices," *Adv. Mater.*, vol. 28, no. 13, pp. 2533–2539, Apr. 2016.

[13] S. Tao, X. Yuan, and J. Lin, "Sequence of focused optical vortices generated by a spiral fractal zone plate," *Appl. Phys. Lett.*, vol. 89, no. 3, pp. 1758–1767, 2006.

[14] A. Ostrovsky, C. Rickenstorff, and V. Arrizon, "Generation of the perfect optical vortex using a liquid crystal spatial light modulator," *Opt. Lett.*, vol. 38, no. 4, pp. 534–536, 2013.

[15] Z. Guo, S. Qu, and S. Liu, "Generating optical vortex with computer-generated hologram fabricated inside glass by femtosecond laser pulses," *Opt. Commun.*, vol. 273, no. 1, pp. 286–289, May 2007.

[16] A. Carpentier, H. Michinel, and J. Salgueiro, "Makling optical vortices with computer-generated holograms," *Amer. J. Physicsi*, vol. 76, no. 10, pp. 916–921, 2008.

[17] D. Cojoc, V. Garbin, E. Ferrari, L. Businaro, F. Romanato, and E. D. Fabrizio, "Laser trapping and micro-manipulation using optical vortices," *Microelectron. Eng.*, vol. 78, pp. 125–131, 2005.

[18] Y. Li, Z. Guo, and S. Qu, "Living cell manipulation in a microfluidic device by femtosecond optical tweezers," *Opt. Lasers Eng.*, vol. 55, pp. 150–154, Oct. 2014.

[19] L. Zhu, "Calculating the torque of the optical vortex tweezer to the ellipsoidal micro-particles," *Opt. Commun.*, vol. 354, pp. 34–39, Nov. 2015.

[20] C. Liu, Z. Guo, and Y. Li, "Manipulating ellipsoidal micro-particles by femtosecond vortex tweezers," *J. Opt.*, vol. 17, no. 3, pp. 988–997, 2015.

[21] G. Rui, X. Wang, and Y. Cui, "Manipulation of metallic nanoparticle with evanescent vortex Bessel beam," *Opt. Exp.*, vol. 23, no. 20, pp. 25707–25716, Sep. 2015.

[22] L. Ran, S. Qu, and Z. Guo, "Surface micro-structures on amorphous alloys induced by vortex femtosecond laser pulses," *Chin. Phys. B*, vol. 19, no. 3, pp. 204–213, 2010.

[23] A. Mair, A. Vaziri, and G. Weihs, "Entanglement of the orbital angular momentum state of photons," *Nature*, vol. 412, no. 6844, pp. 313–316, 2001.

[24] G. Zhong-Yi, Q. Shi-Liang, S. Zheng-He, and L. Shu-Tian, "Superposition of orbital angular momentum of photons by a combined computer-generated hologram fabricated in silica glass with femtosecond laser pulses," *Chin. Phys. B*, vol. 17, no. 11, pp. 4199–4203, 2008.

[25] S. Franke-Arnold, S. M. Barnett, M. J. Padgett, and L. Allen, "Two-photon entanglement of orbital angular momentum states," *Phys. Rev. A, Gen. Phys.*, vol. 65, no. 3, pp. 1337–1348, Feb. 2002.

[26] C. Ku, W. Huang, and J. Huang, "Deterministic synthesis of optical vortices in tailored plasmonic achimedes spiral," *IEEE Photon. J.*, vol. 5, no. 3, pp. 409–419, Jun. 2013.

[27] M. Cheng, "Propagation properties of an optical vortex carried by a Bessel–Guassian beam in anisotropic turbulance," *J. Opt. Soc. Amer. A, Opt. Image Sci.*, vol. 33, no. 8, pp. 1442–1450, 2016.

[28] R. Gaffoglio, A. Cagliero, G. Vecchi, and F. P. Andriulli, "Vortex waves and channel capacity: Hopes and reality," *IEEE Access*, vol. 6, pp. 19814–19822, 2018.

[29] Z. Zhang, S. Zheng, W. Zhang, X. Jin, H. Chi, and X. Zhang, "Experimental demonstration of the capacity gain of plane spiral OAM-based MIMO system," *IEEE Microw. Wireless Compon. Lett.*, vol. 27, no. 8, pp. 757–759, Aug. 2017.

[30] S. Arya and Y. H. Chung, "High-performance and high-capacity ultraviolet communication with orbital angular momentum," *IEEE Access*, vol. 7, pp. 116734–116740, 2019.

[31] F. Tamburini, E. Mari, and A. Sponselli, "Encoding many channels on the same frequency through radio vorticity: First experimental test," *New J. Phys.*, vol. 14, no. 3, pp. 3301–3315, 2012.

[32] W. Park, L. Wang, H.-D. Bruns, D. G. Kam, and C. Schuster, "Introducing a mixed-mode matrix for investigation of wireless communication related to orbital angular momentum," *IEEE Trans. Antennas Propag.*, vol. 67, no. 3, pp. 1719–1728, Mar. 2019.

[33] Y.-M. Zhang and J.-L. Li, "An orbital angular momentum-based array for in-band full-duplex communications," *IEEE Antennas Wireless Propag. Lett.*, vol. 18, no. 3, pp. 417–421, Mar. 2019.

[34] D. Liu, L. Gui, Z. Zhang, H. Chen, G. Song, and T. Jiang, "Multiplexed OAM wave communication with Two-OAM-Mode antenna systems," *IEEE Access*, vol. 7, pp. 4160–4166, 2019.

[35] Y. Zhou, Y. Zhu, Y. Chen, H. Zhao, and W. Xie, "High-speed target imaging for vortex electromagnetic wave radar," *IET Radar, Sonar Navigat.*, vol. 16, no. 2, pp. 306–314, Feb. 2022.

[36] T. Yuan, H. Wang, and Y. Cheng, "Electromagnetic vortex-based imaging using a single receiving antenna: Theory and experimental results," *Sensors*, vol. 17, no. 3, pp. 1–18, 2017.

[37] K. Liu, X. Li, Y. Gao, Y. Cheng, H. Wang, and Y. Qin, "High-resolution electromagnetic vortex imaging based on sparse Bayesian learning," *IEEE Sensors J.*, vol. 17, no. 21, pp. 6918–6927, Nov. 2017.

[38] J. Wang, K. Liu, Y. Cheng, and H. Wang, "Three-dimensional target imaging based on vortex stripmap SAR," *IEEE Sensors J.*, vol. 19, no. 4, pp. 1338–1345, Feb. 2019.

[39] M. Y. Zhao, "Measurement of the rotational Doppler frequency shift of a spinning object using a radio frequency orbital angular momentum beam," *Opt. Lett.*, vol. 41, no. 11, pp. 2549–2552, 2016.

[40] T. Gong, Y. Cheng, X. Li, and D. Chen, "Micromotion detection of moving and spinning object based on rotational Doppler shift," *IEEE Microw. Wireless Compon. Lett.*, vol. 28, no. 9, pp. 843–845, Sep. 2018.

[41] D.-D. Wang, D.-Y. Chen, H.-S. Luan, and H.-L. Peng, "A new method for transcranial vortex microwave beam imaging," in *Proc. Int. Conf. Microw. Millim. Wave Technol. (ICMMT)*, May 2018, pp. 1–3.

[42] G. Turnbull, "The generation of free-space Laguerre–Guassian modes at millimeter-wave frequencies by use of a spiral phaseplate," *Opt. Commun.*, vol. 127, no. 4, pp. 183–188, 1996.

[43] B. Thidé, H. Then, J. Sjöholm, K. Palmer, J. Bergman, T. D. Carozzi, Y. N. Istomin, N. H. Ibragimov, and R. Khamitova, "Utilization of photon orbital angular momentum in the low-frequency radio domain," *Phys. Rev. Lett.*, vol. 99, no. 8, pp. 9892–9905, Aug. 2007.

[44] S. Zhang, X. Wang, M. Wang, H. Peng, B. Wei, and X. Han, "Propagation characteristics of very low frequency vortex electromagnetic waves in an anisotropic ionosphere," *Int. J. Numer. Modelling, Electron. Netw., Devices Fields*, vol. 35, no. 3, pp. 2973–2984, May 2022.

[45] C. Li, L. Wu, and W. Yin, "A dual-polarized and reconfigurable reflectarrya for generation of vortex radio waves," *AIP Adv.*, vol. 8, May 2018, Art. no. 055331.

[46] S. Paek, S. Balasubramanian, S. Kim, and O. Weck, "Small-satellite synthetic aperture radar for continuous global biospheric monitoring: A review," *Remote Sens.*, vol. 12, no. 16, pp. 1–24, 2020.

[47] J. Yang, T. Jin, C. Xiao, and X. Huang, "Compressed sensing imaging: Fundamentals, challenges, and advances," *Sensors*, vol. 19, no. 14, pp. 1–18, 2019.

[48] P. Huang, "Focusing arc-array bistatic synthetic aperture radar based on keystone transform," *Electronics*, vol. 8, no. 12, pp. 1–18, 2019.

[49] H. Zeng, "Broadband terahertz reconfigurable metasurface based on 1-bit asymmetric coding metamaterial," *Opt. Commun.*, vol. 458, no. 1, pp. 1241–1253, 2020.

[50] Y. Hui and W. Wang, "The scattering characteristics of vortex radio-frequency waves in wireless communication," *J. Phys., Conf. Ser.*, vol. 1748, no. 4, pp. 1–8, 2021.

[51] J. Xu, M. Zhao, and R. Zhang, "A wideband F-shaped microstrip antenna," *IEEE Antennas Wireless Propag. Lett.*, vol. 16, pp. 829–832, 2017.

[52] M. Barbuto, F. Trotta, F. Bilotti, and A. Toscano, "Circular polarized patch antenna generating orbital angular momentum," *Prog. Electromagn. Res.*, vol. 148, pp. 23–30, 2014.

[53] C. Guo, X. Zhao, C. Zhu, P. Xu, and Y. Zhang, "An OAM patch antenna design and its array for higher order OAM mode generation," *IEEE Antennas Wireless Propag. Lett.*, vol. 18, no. 5, pp. 816–820, May 2019.

[54] W. Li, "Constructing dual-frequency OAM circular patch antenna using characteristic mode theory," *J. Appl. Phys.*, vol. 126, no. 6, pp. 501–518, 2019.

[55] Z. Zhang, S. Xiao, Y. Li, and B.-Z. Wang, "A circularly polarized multimode patch antenna for the generation of multiple orbital angular momentum modes," *IEEE Antennas Wireless Propag. Lett.*, vol. 16, pp. 521–524, 2017.

[56] W. Dang, "Double-OAM-mode resistor loaded microstrip antenna with a top dielectric layer," *IEICE Electron. Exp.*, vol. 15, no. 12, pp. 895–906, 2018.

[57] F. Shen, J. Mu, K. Guo, and Z. Guo, "Generating circularly polarized vortex electromagnetic waves by the conical conformal patch antenna," *IEEE Trans. Antennas Propag.*, vol. 67, no. 9, pp. 5763–5771, Sep. 2019.

[58] M. Barbuto, F. Bilotti, and A. Toscano, "Patch antenna generating structured fields with a Möbius polarization state," *IEEE Antennas Wireless Propag. Lett.*, vol. 16, pp. 1345–1348, 2017.

[59] S. Zheng, X. Hui, X. Jin, H. Chi, and X. Zhang, "Transmission characteristics of a twisted radio wave based on circular traveling-wave antenna," *IEEE Trans. Antennas Propag.*, vol. 63, no. 4, pp. 1530–1536, Apr. 2015.

[60] Z. Zhang, "Generation of plane spiral OAM waves using traveling-wave circular slot antenna," *IEEE Antennas Wireless Propag. Lett.*, vol. 16, pp. 8–11, 2017.

[61] W. Zhang, "Four-OAM-mode antenna with traveling-wave ring-slot structure," *IEEE Antennas Wireless Propag. Lett.*, vol. 16, pp. 194–197, 2016.

[62] F. Mao, M. Huang, T. Li, J. Zhang, and C. Yang, "Broadband generation of orbital angular momentum carrying beams in RF regimes," *Prog. Electromagn. Res.*, vol. 160, pp. 19–27, 2017.

[63] D. Weiguo, Z. Yongzhong, Y. Yang, and Z. Kaiwei, "A miniaturized dual-orbital-angular-momentum (OAM)–mode helix antenna," *IEEE Access*, vol. 6, pp. 57056–57060, 2018.

[64] Z. Yi, S. Tian, Y. Liu, S. Xiao, H. Tang, K. Kang, and Y. Wu, "Multimode orbital angular momentum antenna based on four-arm planar spiral," *Electron. Lett.*, vol. 55, no. 16, pp. 875–876, Aug. 2019.

[65] L. Wang, H. Chen, and K. Guo, "An inne-and outer-fed dual-arm archimedian spiral antenna for generating multiple orbiral angular momentum modes," *Electronics*, vol. 8, no. 2, pp. 1–16, 2019.

[66] F. Shen, J. Mu, K. Guo, S. Wang, and Z. Guo, "Generation of continuously variable-mode vortex electromagnetic waves with three-dimensional helical antenna," *IEEE Antennas Wireless Propag. Lett.*, vol. 18, no. 6, pp. 1091–1095, Jun. 2019.

[67] Y. Yang, K. Guo, F. Shen, Y. Gong, and Z. Guo, "Generating multiple OAM based on a nested dual-arm spiral antenna," *IEEE Access*, vol. 7, pp. 138541–138547, 2019.

[68] B. Cheo, V. Rumsey, and W. Welch, "A solution to the frequency-independent antenna problem," *IRE Trans. Antennas Propag.*, vol. AP-9, no. 6, pp. 527–534, Nov. 1961.

[69] R. Sivan-Sussman, "Various modes of the equiangular spiral antenna," *IEEE Trans. Antennas Propag.*, vol. AP-11, no. 5, pp. 533–539, Sep. 1963.

[70] S. Mohammadi, "Orbital angular momentum in radio—A system study," *IEEE Trans. Antennas Propag.*, vol. 58, no. 2, pp. 565–572, Feb. 2010.

[71] B. Liu, Y. Cui, and R. Li, "A broadband dual-polarized dual-OAM-mode antenna array for OAM communication," *IEEE Antennas Wireless Propag. Lett.*, vol. 16, pp. 744–747, 2017.

[72] Q. Bai, A. Tennant, and B. Allen, "Experimental circular phased array for generating OAM radio beams," *Electron. Lett.*, vol. 50, no. 20, pp. 1414–1415, 2014.

[73] W. Wei, K. Mahdjoubi, C. Brousseau, and O. Emile, "Generation of OAM waves with circular phase shifter and array of patch antennas," *Electron. Lett.*, vol. 51, no. 6, pp. 442–443, 2015.

[74] F. Spinello, E. Mari, M. Oldoni, R. A. Ravanelli, C. G. Someda, F. Tamburini, F. Romanato, P. Coassini, and G. Parisi, "Experimental near field OAM-based communication with circular patch array," 2015, *arXiv:1507.06889*.

[75] C. J. Deng, K. Zhang, and Z. H. Feng, "Generating and measuring tunable orbital angular momentum radio beams with digital control method," *IEEE Trans. Antenn. Propag.*, vol. 65, no. 2, pp. 899–902, Feb. 2017.

[76] Z. Guo and G.-M. Yang, "Radial uniform circular antenna array for dual-mode OAM communication," *IEEE Antennas Wireless Propag. Lett.*, vol. 16, pp. 404–407, 2017.

[77] H. Li, L. Kang, F. Wei, Y.-M. Cai, and Y.-Z. Yin, "A low-profile dual-polarized microstrip antenna array for dual-mode OAM applications," *IEEE Antennas Wireless Propag. Lett.*, vol. 16, pp. 3022–3025, 2017.

[78] Q. Liu, Z. N. Chen, Y. Liu, F. Li, Y. Chen, and Z. Mo, "Circular polarization and mode reconfigurable wideband orbital angular momentum patch array antenna," *IEEE Trans. Antennas Propag.*, vol. 66, no. 4, pp. 1796–1804, Apr. 2018.

[79] Y.-Y. Wang, Y.-X. Du, L. Qin, and B.-S. Li, "An electronically mode reconfigurable orbital angular momentum array antenna," *IEEE Access*, vol. 6, pp. 64603–64610, 2018.

[80] L. Kang, H. Li, J. Zhou, S. Zheng, and S. Gao, "A mode-reconfigurable orbital angular momentum antenna with simplified feeding scheme," *IEEE Trans. Antennas Propag.*, vol. 67, no. 7, pp. 4866–4871, Jul. 2019.

[81] K. Bi, J. Xu, and D. Yang, "Generation of orbital angular momentum beam with circular polarization ceramic antenna array," *IEEE Photon. J.*, vol. 11, no. 2, pp. 508–515, Apr. 2019.

[82] R. Xi, H. Liu, and L. Li, "Generation and analysis of high-gain orbital angular momentum vortex wave using circular array and parasitic EBG with oblique incidence," *Sci. Rep.*, vol. 7, no. 1, Dec. 2017, Art. no. 17363.

[83] X.-D. Bai, X.-L. Liang, Y.-T. Sun, P.-C. Hu, Y. Yao, K. Wang, J.-P. Geng, and R.-H. Jin, "Experimental array for generating dual circularly-polarized dual-mode OAM radio beams," *Sci. Rep.*, vol. 7, no. 1, Jan. 2017, Art. no. 40099.

[84] F. Qin, L. Li, Y. Liu, W. Cheng, and H. Zhang, "A four-mode OAM antenna array with equal divergence angle," *IEEE Antennas Wireless Propag. Lett.*, vol. 18, no. 9, pp. 1941–1945, Sep. 2019.

[85] Y. H. Cho and W. J. Byun, "Analysis of a uniform rectangular array for generation of arbitrary orbital angular momentum (OAM) modes," *Electron. Lett.*, vol. 55, no. 9, pp. 503–504, May 2019.

[86] Y. Gong, R. Wang, B. Zhang, N. Wang, N. Li, P. Wang, and Y. Deng, "Generation and transmission of OAM-carrying vortex beams using circular antenna array," *IEEE Trans. Antennas Propag.*, vol. 65, no. 6, pp. 2940–2949, Jun. 2017.

[87] C. Deng, W. Chen, Z. Zhang, Y. Li, and Z. Feng, "Generation of OAM radio waves using circular vivaldi antenna array," *Int. J. Antennas Propag.*, vol. 2013, pp. 1–7, Apr. 2013.

[88] T. Yang, D. Yang, B. Wang, and J. Hu, "Experimentally validated, wideband, compact, OAM antennas based on circular vivaldi antenna array," *Prog. Electromagn. Res. C*, vol. 80, pp. 211–219, 2018.

[89] X. Bai, "Generation of OAM radio waves with three polarizations using circular horn antenna array," *IEEE Eur. Conf. Antennas Propag., Lisbon, Portugal*, Apr. 2015, pp. 1–6.

[90] K. Liu, "Generation of OAM beams using phased array in the microwave band," *IEEE Trans. Antennas Propag.*, vol. 64, no. 9, pp. 3850–3857, Sep. 2016.

[91] Y. Yang, J. Xu, H. Yin, W. Bo, J. Tang, J. Ma, J. Xie, and Y. Gong, "Study of a water-immersed orbital angular momentum circular antenna array," in *Proc. IEEE Int. Symp. Antennas Propag. USNC/URSI Nat. Radio Sci. Meeting*, Jul. 2018, pp. 527–528.

[92] C. Xu, "Free-space radio communication employing OAM multiplexing based on Rotman lens," *IEEE Microw. Wireless Compon. Lett.*, vol. 26, no. 9, pp. 738–740, Sep. 2016.

[93] M. R. Akram, L. Gui, and D. Liu, "OAM radio waves generation using dielectric resonator antenna array," in *Proc. Asia–Pacific Int. Symp. Electromagn. Compat. (APEMC)*, May 2016, pp. 591–593.

[94] J. Y. Yin, J. Ren, L. Zhang, H. Li, and T. J. Cui, "Microwave vortex-beam emitter based on spoof surface plasmon polaritons," *Laser Photon. Rev.*, vol. 12, no. 3, Mar. 2018, Art. no. 1600316.

[95] L. Li and X. Zhou, "Mechanically reconfigurable single-arm spiral antenna array for generation of broadband circularly polarized orbital angular momentum vortex waves," *Sci. Rep.*, vol. 8, no. 1, p. 5128, Mar. 2018.

[96] N. Yu, P. Genevet, M. A. Kats, F. Aieta, J.-P. Tetienne, F. Capasso, and Z. Gaburro, "Light propagation with phase discontinuities: Generalized laws of reflection and refraction," *Science*, vol. 334, no. 6054, pp. 333–337, Oct. 2011.

[97] H. C. Zhang, Q. Zhang, J. F. Liu, W. Tang, Y. Fan, and T. J. Cui, "Smaller-loss planar SPP transmission line than conventional microstrip in microwave frequencies," *Sci. Rep.*, vol. 6, no. 1, Mar. 2016, Art. no. 23396.

[98] S. Yu, L. Li, G. Shi, C. Zhu, and Y. Shi, "Generating multiple orbital angular momentum vortex beams using a metasurface in radio frequency domain," *Appl. Phys. Lett.*, vol. 108, no. 24, Jun. 2016, Art. no. 241901.

[99] S. Yu, L. Li, G. Shi, C. Zhu, X. Zhou, and Y. Shi, "Design, fabrication, and measurement of reflective metasurface for orbital angular momentum vortex wave in radio frequency domain," *Appl. Phys. Lett.*, vol. 108, no. 12, Mar. 2016, Art. no. 121903.

[100] S. Yu, L. Li, and G. Shi, "Dual-polarization and dual-mode orbital angular momentum radio vortex beam generated by using reflective metasurface," *Appl. Phys. Exp.*, vol. 9, no. 8, Aug. 2016, Art. no. 082202.

[101] S. Yu, L. Li, and N. Kou, "Generation, reception and separation of mized-state orbital angular momentum vortex beams using metasurfaces," *Opt. Mater. Exp.*, vol. 7, no. 9, pp. 3312–3321, 2017.

[102] X.-S. Meng, J.-J. Wu, Z.-S. Wu, T. Qu, and L. Yang, "Design of multiple-polarization reflectarray for orbital angular momentum wave in radio frequency," *IEEE Antennas Wireless Propag. Lett.*, vol. 17, no. 12, pp. 2269–2273, Dec. 2018.

[103] X. Meng, "Dual-polarized reflect array for generating dual beams with two different orbital angular momentum modes based on independent feeds in C- and X-bands," *Opt. Exp.*, vol. 26, no. 18, pp. 23185–23195, 2018.

[104] G.-T. Chen, Y.-C. Jiao, and G. Zhao, "A reflectarray for generating wideband circularly polarized orbital angular momentum vortex wave," *IEEE Antennas Wireless Propag. Lett.*, vol. 18, no. 1, pp. 182–186, Jan. 2019.

[105] Y. Shen, J. Yang, H. Meng, W. Dou, and S. Hu, "Generating millimeter-wave Bessel beam with orbital angular momentum using reflective-type metasurface inherently integrated with source," *Appl. Phys. Lett.*, vol. 112, no. 14, Apr. 2018, Art. no. 141901.

[106] J. Wu, Z. Zhang, X. Ren, Z. Huang, and X. Wu, "A broadband electronically mode-reconfigurable orbital angular momentum metasurface antenna," *IEEE Antennas Wireless Propag. Lett.*, vol. 18, no. 7, pp. 1482–1486, Jul. 2019.

[107] H. Xu, "Broadband vortex beam generation using multimode pancharatnam-berry metasurface," *IEEE Trans. Antennas Propag.*, vol. 65, no. 12, pp. 7378–7382, Dec. 2017.

[108] Y. Zhang, Y. Lyu, H. Wang, X. Zhang, and X. Jin, "Transforming surface wave to propagating OAM vortex wave via flat dispersive metasurface in radio frequency," *IEEE Antennas Wireless Propag. Lett.*, vol. 17, no. 1, pp. 172–175, Jan. 2018.

[109] X. Dong, H. Sun, C. Q. Gu, Z. Li, X. Chen, and B. Xu, "Generation of ultra-wideband multi-mode vortex waves based on monolayer reflective metasurface," *Prog. Electromagn. Res. M*, vol. 80, pp. 111–120, 2019.

[110] Z. Akram, X. Li, Z. Qi, A. Aziz, L. Yu, H. Zhu, X. Jiang, and X. Li, "Broadband high-order OAM reflective metasurface with high mode purity using subwavelength element and circular aperture," *IEEE Access*, vol. 7, pp. 71963–71971, 2019.

[111] H.-F. Huang and S.-N. Li, "High-efficiency planar reflectarray with small-size for OAM generation at microwave range," *IEEE Antennas Wireless Propag. Lett.*, vol. 18, no. 3, pp. 432–436, Mar. 2019.

[112] C. Ji, J. Song, C. Huang, X. Wu, and X. Luo, "Dual-band vortex beam generation with different OAM modes using single-layer metasurface," *Opt. Exp.*, vol. 27, no. 1, pp. 34–44, Jan. 2019.

[113] Z. Yin, "Tunable beam steeing, focusing and generating of orbital angular momentum vortex beams using high-order patch array," *Appl. Sci.*, vol. 9, no. 15, pp. 1–17, 2019.

[114] Y. Tan, L. Li, and H. Ruan, "An efficient approach to generate microwave vector-vortex fields based on metasurface," *Microw. Opt. Technol. Lett.*, vol. 57, no. 7, pp. 1708–1713, Jul. 2015.

[115] N. Kou, S. Yu, and L. Li, "Generation of high-order Bessel vortex beam carrying orbital angular momentum using multilayer amplitude-phase-modulated surfaces in radio frequency domain," *Appl. Phys. Exp.*, vol. 10, no. 1, 2017, Art. no. 016701.

[116] F. Qin, L. Wan, L. Li, H. Zhang, G. Wei, and S. Gao, "A transmission metasurface for generating OAM beams," *IEEE Antennas Wireless Propag. Lett.*, vol. 17, no. 10, pp. 1793–1796, Aug. 2018.

[117] F. Qin, S. Gao, W.-C. Cheng, Y. Liu, H.-L. Zhang, and G. Wei, "A high-gain transmitarray for generating dual-mode OAM beams," *IEEE Access*, vol. 6, pp. 61006–61013, 2018.

[118] J. Yi, D. Li, R. Feng, B. Ratni, Z. H. Jiang, A. D. Lustrac, D. H. Werner, and S. N. Burokur, "Design and validation of a metasurface lens for converging vortex beams," *Appl. Phys. Exp.*, vol. 12, no. 8, Aug. 2019, Art. no. 084501.
[119] M. L. Chen, L. J. Jiang, and W. E. I. Sha, "Ultrathin complementary metasurface for orbital angular momentum generation at microwave frequencies," *IEEE Trans. Antennas Propag.*, vol. 65, no. 1, pp. 396–400, Jan. 2017.
[120] M. L. N. Chen, L. J. Jiang, and W. E. I. Sha, "Detection of orbital angular momentum with metasurface at microwave band," *IEEE Antennas Wireless Propag. Lett.*, vol. 17, no. 1, pp. 110–113, Jan. 2018.
[121] X. Wang, Y. Chen, S. Zheng, and X. Zhang, "Reconfigurable OAM antenna based on sub-wavelength phase modulation structure," *IET Microw., Antennas Propag.*, vol. 12, no. 3, pp. 354–359, Feb. 2018.
[122] M. R. Akram, X. Bai, R. Jin, G. A. E. Vandenbosch, M. Premaratne, and W. Zhu, "Photon spin Hall effect-based ultra-thin transmissive metasurface for efficient generation of OAM waves," *IEEE Trans. Antennas Propag.*, vol. 67, no. 7, pp. 4650–4658, Jul. 2019.
[123] Y. Wang, K. Zhang, Y. Yuan, X. Ding, G. Yang, J. Fu, and Q. Wu, "Generation of high-efficiency vortex beam carrying OAM mode based on miniaturized element frequency selective surfaces," *IEEE Trans. Magn.*, vol. 55, no. 10, pp. 1–4, Oct. 2019.
[124] K. Liu, G. Wang, Z. Li, W. Guo, Y. Zhuang, and G. Liu, "A multifunctional vortex beam generator based on transparent anisotropic metasurface," *Opt. Commun.*, vol. 435, pp. 311–318, Mar. 2019.
[125] L. Ma, C. Chen, L. Zhou, S. Jiang, and H. Zhang, "Single-layer transmissive metasurface for generating OAM vortex wave with homogeneous radiation based on the principle of Fabry–Pérot cavity," *Appl. Phys. Lett.*, vol. 114, no. 8, Feb. 2019, Art. no. 081603.
[126] L. Guan, Z. He, D. Ding, Y. Yu, W. Zhang, and R. Chen, "Polarization-controlled shared-aperture metasurface for generating a vortex beam with different modes," *IEEE Trans. Antennas Propag.*, vol. 66, no. 12, pp. 7455–7459, Dec. 2018.
[127] M. L. N. Chen, L. J. Jiang, and W. E. I. Sha, "Artificial perfect electric conductor-perfect magnetic conductor anisotropic metasurface for generating orbital angular momentum of microwave with nearly perfect conversion efficiency," *J. Appl. Phys.*, vol. 119, no. 6, Feb. 2016, Art. no. 064506.
[128] X. Meng, J. Wu, Z. Wu, L. Yang, L. Huang, X. Li, T. Qu, and Z. Wu, "Generation of multiple beams carrying different orbital angular momentum modes based on anisotropic holographic metasurfaces in the radio-frequency domain," *Appl. Phys. Lett.*, vol. 114, no. 9, Mar. 2019, Art. no. 093504.
[129] X. Meng, "Design, fabrication, and measurement of an anisotropic holographic metasurface for generating vortex beams carrying orbital angular momentum," *Opt. Lett.*, vol. 44, no. 6, pp. 1452–1455, 2019.
[130] J. Q. Han, L. Li, H. Yi, and Y. Shi, "1-bit digital orbital angular momentum vortex beam generator based on a coding reflective metasurface," *Opt. Mater. Exp.*, vol. 8, no. 11, pp. 3470–3478, 2008.
[131] J. Han, L. Li, H. Yi, and W. Xue, "Versatile orbital angular momentum vortex beam generator based on reconfigurable reflective metasurface," *Jpn. J. Appl. Phys.*, vol. 57, no. 12, Dec. 2018, Art. no. 120303.
[132] D. Zhang, X. Cao, H. Yang, and J. Gao, "Radiation performance synthesis for OAM vortex wave generated by reflective metasurface," *IEEE Access*, vol. 6, pp. 28691–28701, 2018.
[133] D. Zhang, "Multiple OAM vortex beams generation using 1-bit metasurface," *Opt. Exp.*, vol. 26, no. 19, pp. 24804–24815, 2018.
[134] D. Zhang, X. Cao, J. Gao, H. Yang, W. Li, T. Li, and J. Tian, "A shared aperture 1 bit metasurface for orbital angular momentum multiplexing," *IEEE Antennas Wireless Propag. Lett.*, vol. 18, no. 4, pp. 566–570, Apr. 2019.
[135] L. Zhang, S. Liu, L. Li, and T. J. Cui, "Spin-controlled multiple pencil beams and vortex beams with different polarizations generated by pancharatnam-berry coding metasurfaces," *ACS Appl. Mater. Interface*, vol. 9, no. 41, pp. 36447–36455, Oct. 2017.
[136] Q. Ma, "Beam-editing coding metasurfaces based on polarization bit and orbital-angular-momentum-mode bit," *Adv. Opt. Mater.*, vol. 5, no. 23, 2017, Art. no. 1700548.
[137] R. Y. Wu, L. Zhang, L. Bao, L. W. Wu, Q. Ma, G. D. Bai, H. T. Wu, and T. J. Cui, "Digital metasurface with phase code and reflection–transmission amplitude code for flexible full-space electromagnetic manipulations," *Adv. Opt. Mater.*, vol. 7, no. 8, Apr. 2019, Art. no. 1801429.

OMAR A. SARAEREH received the B.S. degree in telecommunication engineering from Mutah University, Jordan, in 1999, the M.Sc. degree in digital communication systems in the U.K., and the Ph.D. degree in electrical and electronic engineering/mobile communications from Loughborough University, Loughborough, U.K., in 2005. From 2001 to 2005, he was a member of staff with the Centre for Mobile Communication Research, Loughborough University. He is currently a Full Professor with the Department of Electrical Engineering, The Hashemite University, Jordan. He has more than 17 years of academic and practical experience in electrical engineering, mobile communications, various antennas design, fabrication and measurements, radiation hazards and health effects, and wireless communications. He was a high-level consultant and a turnkey solution originator in countless business and charitable sectors, and an international public speaker and a trainer on a variety of business and people management topics. He has published many articles in various international journals and conferences.